AIP Publishing

This manuscript was accepted by J. Chem. Phys. Click here to see the version of record.

Microscopic origin of the charge transfer in single crystals based on thiophene derivatives: a combined NEXAFS and density functional theory approach

A. Chernenkaya,[1,2] A. Morherr,[3] S. Backes,[4] W. Popp,[4] S. Witt,[3] X. Kozina,[2] S. A. Nepijko,[2] M. Bolte,[5] K. Medjanik,[6] G. Öhrwall,[6] C. Krellner,[3] M. Baumgarten,[7] H. J. Elmers,[2] G. Schönhense,[2] H. O. Jeschke,[4] and R. Valentí[4]

[1)] *Graduate School Materials Science in Mainz, 55128 Mainz, Germany*
[2)] *Institut für Physik, Johannes Gutenberg-Universität, 55099 Mainz, Germany*[a)]
[3)] *Physikalisches Institut, Goethe-Universität, 60438 Frankfurt am Main, Germany*
[4)] *Institut für Theoretische Physik, Goethe-Universität, 60438 Frankfurt am Main, Germany*
[5)] *Institut für Anorganische Chemie, Goethe-Universität, 60438 Frankfurt am Main, Germany*
[6)] *Lund University, MAX-IV Laboratory, 22100 Lund, Sweden*
[7)] *Max-Planck-Institut für Polymerforschung, 55021 Mainz, Germany*

(Dated: 29 June 2016)

We have investigated the charge transfer mechanism in single crystals of DTBDT-TCNQ and DTBDT-F_4TCNQ, (where DTBDT is dithieno[2,3-d;2′,3′-d′] benzo[1,2-b;4,5-b′]dithiophene), using a combination of near-edge X-ray absorption spectroscopy (NEXAFS) and density functional theory calculations (DFT) including final state effects beyond the sudden state approximation. In particular, we find that a description that considers the partial screening of the electron-hole Coulomb correlation on a static level as well as the rearrangement of electronic density shows excellent agreement with experiment and allows to uncover the details of the charge transfer mechanism in DTBDT-TCNQ and DTBDT- F_4TCNQ, as well as a reinterpretation of previous NEXAFS data on pure TCNQ. Finally, we further show that almost the same quality of agreement between theoretical results and experiment is obtained by the much faster $Z+1/2$ approximation, where the core hole effects are simulated by replacing N or F with atomic number Z with the neighboring atom with atomic number $Z+1/2$.

Keywords: Charge-transfer complex, NEXAFS, F_4TCNQ, TCNQ, thiophene, DTBDT

I. INTRODUCTION

Novel charge-transfer (CT) compounds based on low-dimensional organic materials with π-conjugated rings decorated with different ligands offer a huge potential for variability and unconventional behavior in materials research. The design of new organic molecules and their combinations provide compounds with unusual properties like superconductivity, magnetism, spin density waves or charge density waves[1]. Many of the organic conductors and superconductors are based on the bis(ethylenedithio)tetrathiafulvalene (BEDT-TTF) donor combined with various acceptors[2,3]. In this context, polycyano derivatives have mainly been used as acceptors like tetracyanoquinodimethane (TCNQ)[1,4]. Such systems are very promising in potential applications in organic electronics and solar cell systems[5].

On the other hand, P-type organic semiconductors are indispensable for diodes and complementary circuits with a high operation speed and low power consumption and which are widely represented by oligo- and polythiophenes[6]. The interest on such building blocks for complex electronic systems is due to the high polarizability of the sulfur atoms in thiophenes leading to a stabilization of the whole molecular system and excellent charge carrier transport[7]. Furthermore, a possible tuning of electronic properties can be achieved by varying the structural particularities.

Charge transfer complexes are also interesting from the fundamental research perspective as model systems with new electronic states in comparison to pure donor and acceptor phases. A few examples of CT complexes have been intensively investigated in the past focusing mainly on the electronic structure[8–12].

Recently, a new class of donors represented by derivatives of the compound dithieno[2,3-d;2′,3′-d′]benzo[1,2-b;4,5-b′]dithiophene, abbreviated as DTBDT (Fig. 1) were synthesized[13]. Based on this precursor with alkyl groups, thin films of the CT mixture DTBDT-F_4TCNQ have been obtained by molecular beam epitaxy in ultra-high vacuum and characterized by scanning tunneling microscopy[14].

As it has been shown in a few studies on organic complexes[15–20] NEXAFS (near edge X-ray absorption fine structure) spectroscopy[21,22] is a powerful method for investigating the orbital-resolved charge transfer process. Furthermore, this method is not surface-sensitive and not destructive. The rather large probing depth of 3-5

[a)] Electronic mail: chernenk@uni-mainz.de

ACCEPTED MANUSCRIPT

This manuscript was accepted by J. Chem. Phys. Click here to see the version of record.

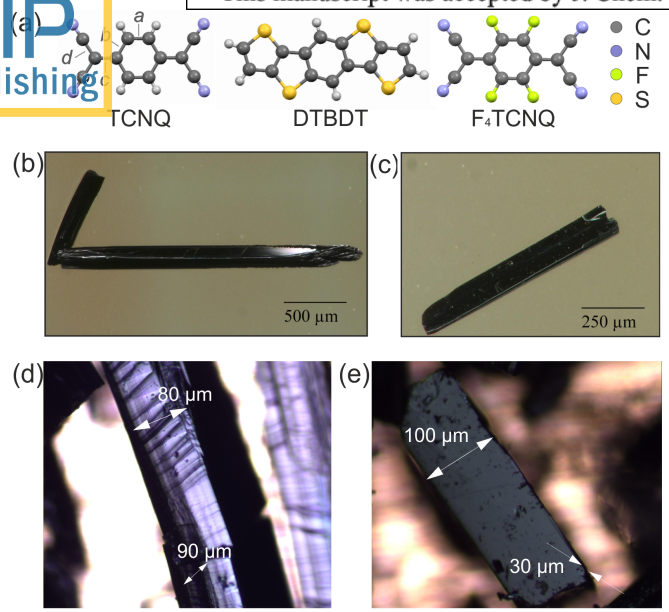

FIG. 1. (a) Molecular structures of the thiophene based donor DTBDT and acceptors TCNQ and F_4TCNQ. Bond lengths a, b, c, and d are shown for the TCNQ molecule that directly correlate with the charge transfer in the complex (see the text); (b) needle-shaped crystals of DTBDT-TCNQ and (c) DTBDT-F_4TCNQ, grown by gas-phase crystallization; orientation on the sample holder of (d) DTBDT-TCNQ and (e) DTBDT-F4TCNQ crystals with marked dimensions during NEXAFS measurements.

nm and instrumental resolution better than 30 meV allows for the ability to follow the change in occupancy of molecular orbitals and therefore facilitates a very precise analysis of the electronic structure in an orbital selective manner[17]. Theoretically, the calculation of X-ray absorption spectra has a long history[23,24]. Slaters transition state method[25] has been used in calculations of core to π^* excitation energies of small molecules[26] and in quantum chemical NEXAFS studies[27]. The half-core hole method has been applied in calculations for large molecules[28]. In periodic density functional calculations, X-ray absorption spectroscopy has for example been studied for ice and water[29]. X-ray absorption spectra can be calculated within popular plane wave codes[30,31]. Recently, the determination of core level spectra via Bethe-Salpeter equations has been introduced into a multiple-scattering code[32].

In this work we present combined NEXAFS measurements with density functional theory (DFT) calculations[33,34] for gas-phase crystallized molecular crystals of donor DTBDT in combination with two acceptors of different strength: TCNQ and F_4TCNQ (see Fig. 1 for details of the crystals). Our results show clearly that in order to interpret NEXAFS observations final state effects have to be taken into account in the calculations; this leads to some changes in peak assignment compared to previous studies[35] relying on the initial state approximation for the interpretation of NEXAFS spectra. The discussion of charge transfer complex formation is based on a quantitative comparison of the measurements and the DFT calculations in several different approximations. Since NEXAFS measurements give direct access to the unoccupied electronic states of the material, it is possible to compare and discuss even subtle changes and differences in the electronic structure due to the charge transfer process.

II. EXPERIMENTAL METHODS

The DTBDT donor molecules were synthesized as described in Ref.[13]. Acceptor molecules TCNQ and F_4TCNQ were commercially available (Fisher Scientific, TCI).

Single crystals of the CT compounds were grown by physical vapor transport[36,37]. The starting materials, 6 mg of DTBDT and 8 mg of TCNQ or F_4TCNQ, were ground together and transferred into a glass ampoule, which was cleaned by ethanol and acetone and baked in a box furnace for at least 24 hours to remove water. The glass ampoule was evacuated ($p \sim 10^{-3}$ mbar), sealed and placed into a horizontal oven with a temperature gradient. The source material was positioned at the hottest zone at around 225°C. Dark, needle-shaped CT crystals form at 190-200°C. The growth procedure lasted ∼50 hours and the ampoule was removed from the hot oven after the starting material was completely sublimated. The ampoule was opened and the dark needles were collected from the walls (Fig. 1). The structure of the single crystals was determined by X-ray diffraction. Results of the crystal structure of DTBDT-TCNQ and DTBDT-F_4TCNQ are presented in Fig. 2 and Table I and in more detail in the Supplementary Materials

Infrared (IR) spectroscopy was carried out on polycrystalline samples of DTBDT-TCNQ and DTBDT-F_4TCNQ and compared to spectra recorded from powders of pure acceptors TCNQ and F_4TCNQ, respectively. Spectra were obtained using a Nicolet 730 FT-IR spectrometer between 4000 and 500 cm^{-1} at room temperature. Resolution of the measurements was 1 cm^{-1}.

The NEXAFS measurements were performed at the soft X-ray beamline I1011 at MAX II, Lund (Sweden), at an energy resolution of 120 meV and 200 meV for N 1s and F 1s, respectively, where the drain current from the sample was recorded. The total electron yield originated from a subsequent Auger process that neutralizes the core hole and led to the emission of Auger electrons which in a secondary process were transformed into slow secondary electrons. The information depth was about 5 nm, corresponding to approximately 15 molecular layers, which was sufficient for yielding information on the bulk of the crystallites.

Because the charge transfer process mainly alters the unoccupied states of the acceptor, we have investigated nitrogen and fluorine K-edge spectra which are specific

ACCEPTED MANUSCRIPT

This manuscript was accepted by J. Chem. Phys. Click here to see the version of record.

AIP Publishing

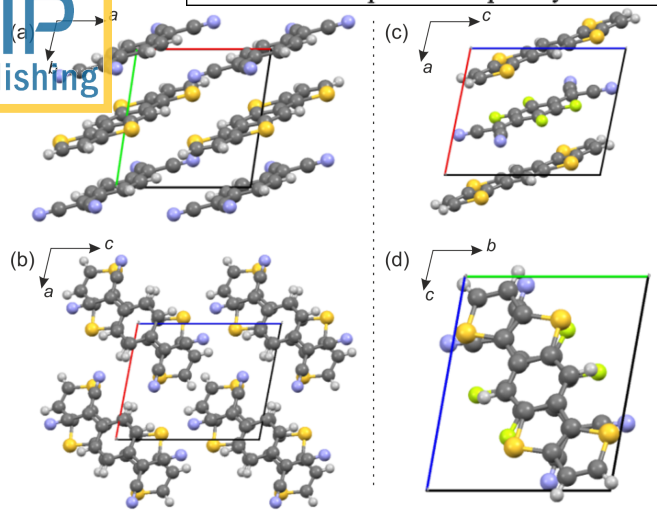

FIG. 2. Overview of the crystal structures of DTBDT-TCNQ (left) and DTBDT-F_4TCNQ (right). DTBDT-TCNQ: (a) mixed stack in b direction. (b) view along the b axis; DTBDT-F_4TCNQ: (c) mixed stack in a direction, (d) view along the a axis.

to the acceptor orbitals. Spectra from the mixed phase crystals with DTBDT donor molecules were compared to spectra of the pure acceptor moieties. All measurements were performed for powders of the pure acceptor and donor molecules and for a large number of mixed-phase crystals glued to a copper sample holder at room temperature in different orientations (see Fig. 1 (d) (e)).

III. THEORETICAL METHODS

Based on the experimentally determined crystal structures of TCNQ[38], F_4TCNQ[39], DTBDT-TCNQ and DTBDT-F_4TCNQ, ab-initio calculations were performed using a number of quantum chemistry and density functional theory codes. The single molecule gas phase calculations have been carried out with the program package ORCA[40] in the framework of DFT and TDDFT. To this end, the B3LYP functional[41–43] in combination with the Ahlrichs VDZ basis set with (d, p)-polarisation functions and diffuse functions from the aug-cc-pVDZ basis has been utilised[44,45]. The optimised structures of the single molecules were verified by frequency analysis. For the analysis of the NEXAFS spectra of TCNQ and F_4TCNQ molecular crystals, we used the full-potential linearized augmented plane-wave basis (FLAPW) as implemented in the Wien2k package[46]. We calculate NEXAFS spectra using the XSPEC program[47,48] integrated into Wien2k using integer and fractional core holes[49]. The generalized gradient approximation in the Perdew, Burke, Ernzerhof (PBE) form[50] was used. For DFT calculation of TCNQ and F_4TCNQ in the LAPW basis we employed a k-mesh of dimension $9 \times 3 \times 9$. We used a value of $R_{KMAX} = R_{mt} \cdot K_{Max} = 7$, which defines the size of the basis set and where R_{mt} is the smallest muffin tin radius and K_{Max} is the largest wave number. The calculation was converged to within 10^{-4} eV accuracy of the total energy and 10^{-5} e of the total charge. Finally, calculations for all molecular crystals discussed in this work were performed using the full potential local orbital (FPLO) basis set[51] and the PBE exchange-correlation functional[50]. Note that FPLO is an all electron fixed basis set method so that the basis set quality does not need to be specified. The self-consistent charge density allowed extracting the charge transfer as determined from the excess charge on TCNQ or F_4TCNQ; due to the expansion in terms of local orbitals, a precise local decomposition of the total charge density is possible. A k-mesh of at least $10 \times 10 \times 10$ points was used to converge the electronic structures of all compounds. Convergence of half core hole spectra was checked using $24 \times 24 \times 24$ k meshes.

TABLE I. Crystallographic data for DTBDT-TCNQ and DTBDT-F_4TCNQ crystals.

Crystal data	DTBDT-TCNQ	DTBDT-F_4TCNQ
Chemical formula	$C_{26}H_{10}N_4S_4$	$C_{26}H_6F_4N_4S_4$
Formula weight	506.66	578.59
Crystal system	Triclinic	Triclinic
Space group	P -1	P -1
Unit cell dimensions	a=7.5227(3) Å,	a=7.7585(15) Å,
	b=7.8873(3) Å,	b=7.8305(13) Å,
	c=9.2504(5) Å,	c=9.4063(18) Å,
	α=101.503(3)°,	α=99.027(14)°,
	β=99.140(2)°,	β=100.553(15)°,
	γ=96.410(3)°	γ=94.654(15)°,
Volume	525.15(4) Å^3	551.27(18) Å^3
Z	1	1
Crystal size (mm)	0.080 x 0.110 x 0.420	0.410 x 0.080 x 0.040

IV. RESULTS AND DISCUSSION

A. Crystal structure of DTBDT-TCNQ and DTBDT-F_4TCNQ

The crystal structures of DTBDT, DTBDT-TCNQ and DTBDT-F_4TCNQ were obtained by single-crystal X-ray diffraction. Figure 2 shows the crystal structure of both CT complexes. DTBDT-TCNQ forms mixed stacks along the b-axis and DTBDT-F_4TCNQ forms mixed stacks along the a-axis, where the DTBDT and the TCNQ or F_4TCNQ alternate, respectively. The formation of the mixed-stack structure minimizes the electrostatic energy of the partially ionized donor and acceptor molecules, while covalent intermolecular bonding between DTBDT molecules via the sulphur orbitals plays a less important role. Both crystal structures are triclinic with space group $P\,\bar{1}$. Detailed structural information

ACCEPTED MANUSCRIPT

This manuscript was accepted by J. Chem. Phys. Click here to see the version of record.

about the compounds is provided in the Supplementary Materials section.

B. Infrared spectroscopy

IR spectra of the C≡N stretching vibration were measured at room temperature for pure acceptor powders TCNQ and F_4TCNQ and for crystals of the mixed phases DTBDT-TCNQ and DTBDT-F_4TCNQ. In the mixed crystals of DTBDT-TCNQ (Fig. 3 (a)) the vibration frequency was red-shifted to $\omega_{\mathrm{CT}} = 2213.9$ cm^{-1} with $\omega_0 = 2223.5$ cm^{-1} and $\omega_1 = 2183$ cm^{-1} (in Ref.[52]). Due to the asymmetric line shape, the estimated error of the frequency values was 0.4 cm^{-1}. This is indicative of a charge transfer on the order of 0.24(1) e, determined from eq. (1)[53]:

$$\rho = \frac{2(\omega_0 - \omega_{\mathrm{CT}})}{\omega_0\left(1 - \frac{\omega_1^2}{\omega_0^2}\right)} , \qquad (1)$$

where ω_0, ω_1 and ω_{CT} denote the frequencies of the C≡N stretching modes for neutral acceptor, anion (where ρ=1) and the charge transfer salt, respectively. This equation has been previously applied to both TCNQ and F_4TCNQ acceptors, and other molecules[11,36,54,55] that will serve for comparison cases.

For the DTBDT-F_4TCNQ crystals the vibration frequencies were: $\omega_{\mathrm{CT}} = 2219.8$ cm^{-1}, $\omega_0 = 2227.8$ cm^{-1} and $\omega_1 = 2190$ cm^{-1} according to Ref.[56]. In this case the obtained result for CT was 0.21(1) e (Fig. 3 (b)). The charge transfer is usually proportional to the electron affinity ($E_{e.a.}$) of the acceptor molecule. Therefore, following this simple argument, one would expect a larger charge transfer in the case of the F_4TCNQ ($E_{e.a.} \approx 5.2$ eV) compared to the TCNQ ($E_{e.a.} \approx 4.8$ eV) based compound. In contrast, the IR-spectroscopy suggests the opposite effect, the charge transfer in DTBDT-F_4TCNQ is slightly smaller than in DTBDT-TCNQ. The same inverse dependence of the acceptor electron affinity and the charge transfer was observed by Rudloff et al.[11] on the systems TMP-TCNQ and TMP-F_4TCNQ .

In Table II the experimental values of the charge transfer obtained from infrared spectroscopy and conductivity measurements are compared with theoretical values obtained from DFT[33,34] electronic structure calculations by employing the FPLO[51] basis and the PBE exchange-correlation functional[50]. The charge transfer was obtained in terms of the calculated charges on the atoms. Comparison of the theoretical results with the IR-based values shows a reasonable agreement although the theoretical values follow the expectation of a larger charge transfer for stronger acceptor electron affinity in contrast to the experimental observation. Experimentally, the reversed order is at the limit of uncertainty (error ±0.01). Table II also shows the calculated band gaps between the HOMO of the donor and the LUMO of the acceptor molecule that compare well with those extracted from electronic transport measurements (see Supplementary Materials).

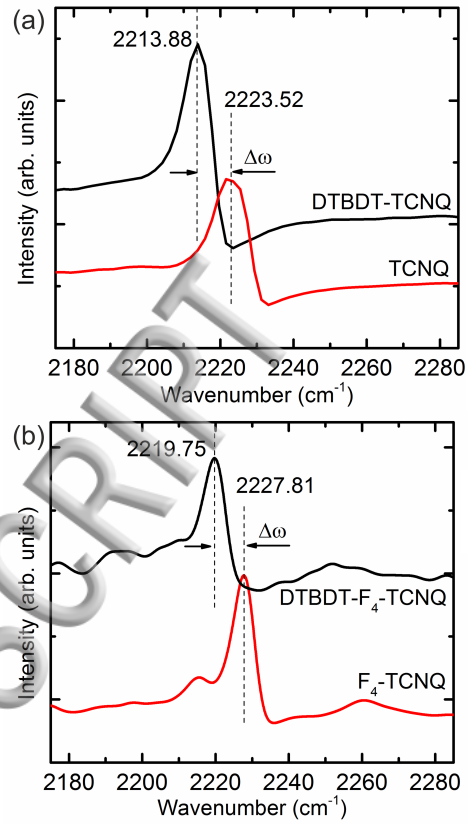

FIG. 3. (a) IR spectra of the C≡N stretching vibration in TCNQ powder and crystals of the CT complex DTBDT-TCNQ; (b) same for F_4TCNQ and DTBDT-F_4TCNQ.

It should be noted that the calculated gap is the distance between the top of the valence band (upper edge of HOMO) and the bottom of the conduction band (lower edge of LUMO). The experimental gap ΔE, determined from the Arrhenius plot agrees very well with the calculated values (see Table 2).

C. Near-edge X-ray absorption fine structure

Experimental results for the nitrogen and fluorine K-edges NEXAFS spectra for DTBDT-TCNQ and DTBDT-F_4TCNQ are shown in Figure 4. Nitrogen and fluorine are exclusively present in the acceptor (see Fig. 1 (a)). Therefore, it is possible to follow the change of the unoccupied charge density distribution of the acceptor upon formation of the complex without interfering with orbitals that are localized at the donor.

The nitrogen K-edge NEXAFS spectra of TCNQ (Fig. 4 (a)) consist of peaks A-D. Note that the major signal (B) is not split into two components as in previous works[17,35], as is evident from theory (see be-

ACCEPTED MANUSCRIPT

AIP Publishing

This manuscript was accepted by J. Chem. Phys. Click here to see the version of record.

TABLE I. Values from DFT calculations for the charge ρ on TCNQ-F_4TCNQ and the band gap for both DTBDT-TCNQ and DTBDT-F_4TCNQ crystals in comparison to experimental values.

	ρ (e)	Charge gap (eV)	ρ (e)	ΔE (eV)
	From DFT calculations		From IR spectroscopy	From transport measurements
DTBDT-TCNQ	0.31	0.48	0.24(1)	0.51(1)
DTBDT-F_4TCNQ	0.36	0.34	0.21(1)	0.36(1)

low). The peak maxima are located at photon energies of 396.21, 398.17, 399.17 and 400.96 eV, respectively, as determined by the fit routine. Comparing the nitrogen K-edge spectra of the DTBDT-TCNQ microcrystals with pure TCNQ (Fig. 4 (a)), two main changes should be noticed: firstly, peak A decreases and broadens. Secondly, the intensity decrease of the high energy tail of peak B masks peak C. In addition, an overall decrease of the absorption intensity is observed, which is attributed to the lower concentration of nitrogen atoms in the mixed compound (16 % less in relation to crystalline TCNQ).

Due to the similar configuration of the cyano groups in TCNQ and F_4TCNQ, their nitrogen K-edge spectra have similar shapes. Therefore, the spectra for F_4TCNQ are also characterized by peaks A-D with slightly shifted positions of the maxima at 395.98, 398.21, 399.35 and 401.25 eV, respectively (Fig. 4 (b)). Similarly to the previous case, in the nitrogen spectra for DTBDT-F_4TCNQ the intensity of the highest peak B is lower due to lower nitrogen content. Peaks A and C have higher intensities, which will be discussed below. Figure 4 (c) shows the fluorine K-edge NEXAFS spectra of DTBDT-F_4TCNQ in comparison to the pure acceptor F_4TCNQ. The spectra consist of peaks F-I and a weak signal E in the low-energy shoulder of peak F. The intensity is decreased in the CT compound for all peaks due to the fluorine abundance.

NEXAFS is a local probe with high chemical selectivity. In NEXAFS the final state has a hole in the core state and an additional electron in the conduction band. In order to provide a detailed interpretation of the NEXAFS measurements we have calculated NEXAFS spectra in the framework of density functional theory (DFT) with four different methods: (i) The so-called *sudden state approximation* or ground state approximation which assumes that the time of the interaction of the X-ray photon with the electronic subsystem is much shorter than the typical timescale for spatial rearrangement of the electronic density. Therefore, the spectra can be calculated in terms of the ground-state (partial nitrogen or fluorine) density of states (DOS). (ii) A method which improves upon the previous plain DFT density of states is the calculation of the excitation spectrum through *time-dependent DFT* (TDDFT)[57,58]. We performed calculations for the molecules with the ORCA package[40]. (iii) A third approach which considers the screening of the electron-hole Coulomb correlation on a static level as well as the rearrangement of electronic density, is the *core-hole (supercell) approximation*. The idea of this approach is to remove one core electron (or a fraction of it) on one atom in the (super-)cell with $P1$ symmetry and add it in the conduction band. In this approach, the double differential scattering cross-section is calculated in the Born approximation[47,48]. We performed these calculations for the molecular crystals with the Wien2k package[46]. These calculations contain the key ingredients of the NEXAFS process but they are computer intensive, therefore (iv) we also tested the so-called *Z+1 approximation* which consists in replacing one N atom (for nitrogen K-edge NEXAFS) or one F atom (for fluorine K-edge NEXAFS) with atomic number Z by the neighboring atom with atomic number Z+1 or Z+1/2 (see Fig. 5). This assumes that the lifetime of the excitation is much longer than the electronic timescale. A compromise between the two end cases (Z versus Z+1) can be obtained by considering a fractional Z+1/2. We performed Z+1 and Z+1/2 calculations with the FPLO code[51].

We first tested the four methods for the pure acceptors TCNQ (see Fig. 6) and F_4TCNQ (see Supplementary Material, Figs. S6 and S7). The spectra obtained in the FLAPW basis are generated via a product of the partial density of states and the corresponding matrix elements and transition probabilities cannot be directly compared to experiment in absolute value. We show therefore the resulting spectra in arbitrary units. A closer look at Fig. 6 shows that the sudden state approximation or plain DFT (case (i)) provides a very poor description of nitrogen K-edge NEXAFS for TCNQ. Neither the N 2p density of states (DOS) on an atom in the molecule (shaded region in Fig. 6 (a)) nor its convoluted form (red line) reproduce the measured NEXAFS spectra. Previous works[15,35] used this approach to identify the origin of the peaks observed in NEXAFS. However, in order to reach a reasonable agreement between theory and experiment, assumptions on energy shifts and on the absence of certain peaks in NEXAFS were necessary.

An improvement upon simple partial N 2p DOS is obtained by calculating the excitation spectrum of the system via TDDFT (Fig. 6 (b)). The dominating peak of the theoretical spectrum (orange curve) is now only 0.55 eV above the experimental peak B and the spectral weights of the peaks agree reasonably well. Including the effect of the screening of one full core hole and corresponding rearrangement of the electronic density (Fig. 6 (c)) (case (iii)) produces the desired four main peaks observed in the NEXAFS spectrum but their positions were not yet well accounted for. However, when we reduce the strength of screening in the calculation by considering only half a core hole (Fig. 6 (d)), we observe an excellent agreement

ACCEPTED MANUSCRIPT

This manuscript was accepted by J. Chem. Phys. Click here to see the version of record.

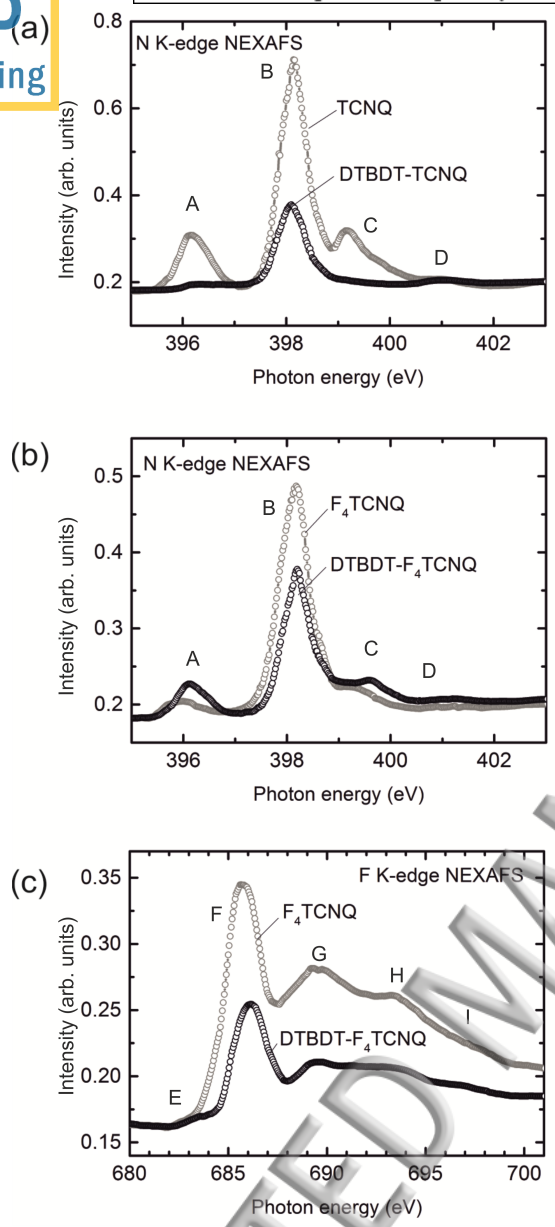

FIG. 4. Nitrogen (a, b) and fluorine (c) K-edge spectra for pure acceptors and the CT complexes investigated in this work. Spectra of pure acceptors are scaled to 1 at maximum intensity, spectra of CT compounds have correct relative intensities accordingly. The intensity changes partly reflect the different atom densities in pure moieties and compounds.

with experiment without further adjustment of parameters. A similar approach has proven successful for atomic calculations where the Slater integrals are reduced with respect to the Hartree-Fock values[59]. This agreement was also observed in all other test cases considered (nitrogen and fluorine K-edge NEXAFS for F_4TCNQ) as shown in the Supplementary Information. This would suggest to consider this approach as the method of choice. These calculations are, however, computer intensive and we performed, as a last test, calculations with the much

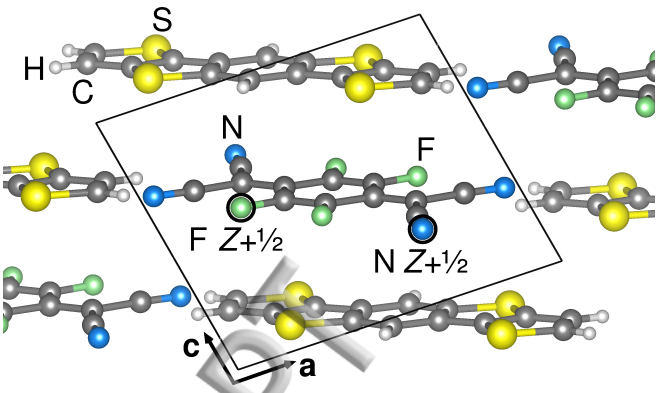

FIG. 5. Positions of the probed nitrogen and fluorine atoms in the CT complex.

faster $Z+1/2$ approximation (case (iv)). This approximation gave for the systems studied here very similar results to the half core-hole approach (compare Figs. 6 (d) and 7 (a)), and we performed all computations hereafter with the $Z+1/2$ method. We aligned experimental and theoretical spectra by choosing an appropriate reference energy $E_{\text{reference}}$. In the case of the experimental spectra, this is the maximum of the first observed peak, which means that $E_{\text{reference}} \approx 396.2$ eV in the case of nitrogen K shell spectra. Note that the precise value of this energy was dependent on the day to day calibration of the photon beam energy, however, varying by not more than 0.5 eV. For the theoretical spectra, $E_{\text{reference}}$ is given by the energy of the lowest unoccupied peak in the density of states, corresponding to the LUMO level.

Figure 7 presents a summary on the comparison between the experimental NEXAFS data for all systems and the calculated spectra obtained with the $Z+1/2$ method. We plotted both, the $2p$ DOS of the $Z+1/2$ atom (shaded regions) as well as the convoluted results (blue lines), assuming a lifetime broadening of $\Gamma = 0.5$ eV for nitrogen and $\Gamma = 1.5$ eV for fluorine. The agreement with the experimental NEXAFS data is remarkable and sets the stage for interpreting the experimental observations.

For the peak assignment we relate in Figs. 8 (a), (b) the TCNQ $Z+1/2$ p DOS (which reproduces the experimental results) with the DOS in TCNQ. Keeping in mind that NEXAFS is a local probe that provides information on the N $2p$ states and through them, of the bonding related to the nitrogen atoms, we observe that the most prominent peak B corresponds directly to the newly created $2p$ state through the core hole excitation (sharp peak at 2.2 eV in Fig. 8 (b)). Peak A corresponds to the LUMO level of TCNQ which is a σ^* resonance originating from the lowest empty orbitals from the cyano groups in the TCNQ molecule. Peaks C and D are directly associated with the higher unoccupied nitrogen $2p$ levels hybridizing with carbon states (a molecular orbital picture of the higher energy levels is unrealistic due to the high delocal-

ACCEPTED MANUSCRIPT

AIP Publishing

This manuscript was accepted by J. Chem. Phys. Click here to see the version of record.

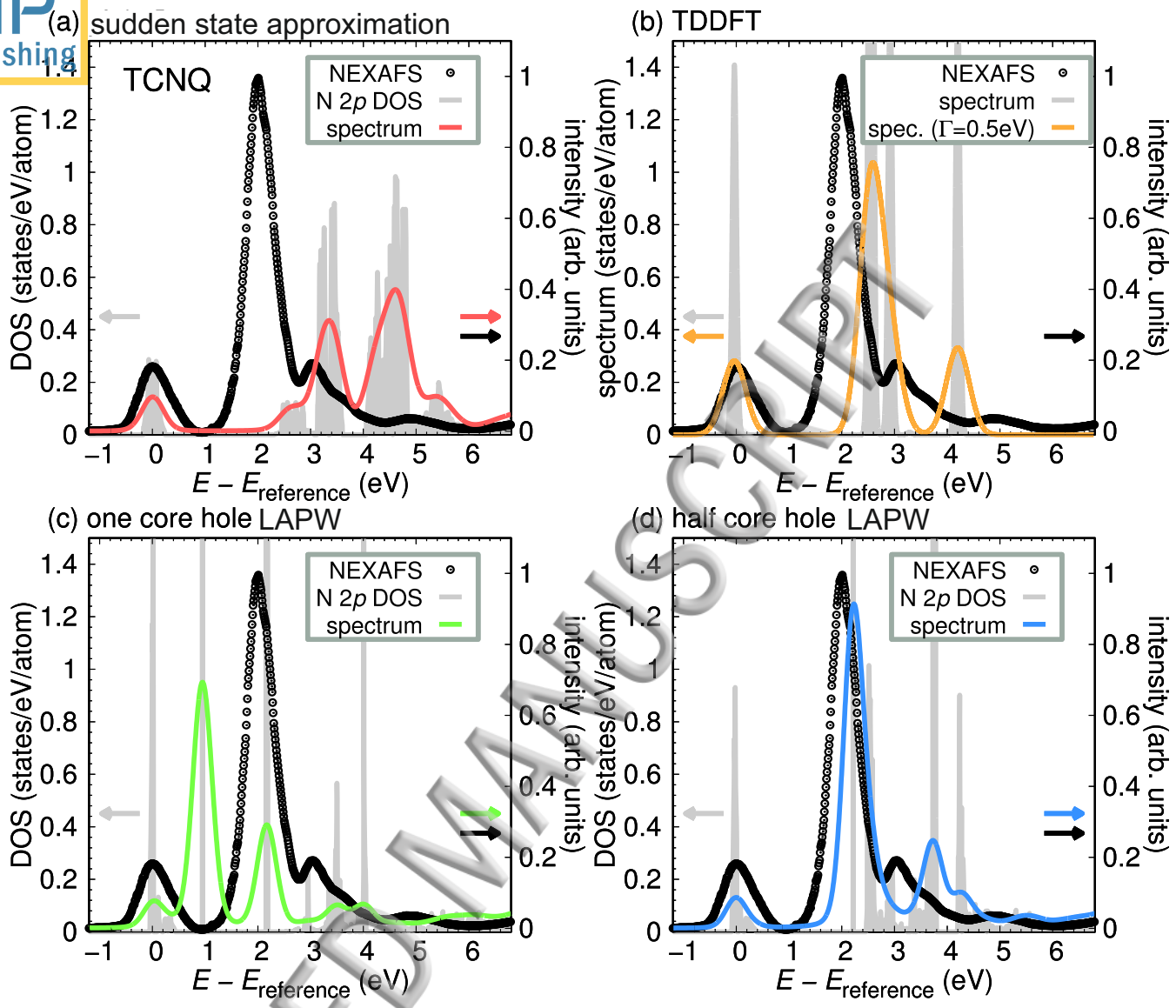

FIG. 6. Nitrogen K-edge spectra for TCNQ calculated with various methods described in the text compared to experimental NEXAFS data (black circles) scaled to 1 at maximum intensity. The spectra (colored curves) in (a), (c), (d) were multiplied by the same factor to make them comparable. The spectrum in (b) was obtained from the DOS by convolution with an assumed half width of $\Gamma = 0.5$ eV. The energy scale is explained in the text.

ACCEPTED MANUSCRIPT

ization of these states). A similar analysis can be done for the acceptor F_4TCNQ (see Supplementary Information, Fig. S8).

In order to identify the peak structure in the compounds, we show in Figs. 8 (c), (d) the comparison between the DOS of DTBDT-TCNQ and the DOS of DTBDT-TCNQ where a nitrogen atom has been substituted by a Z+1/2 atom (see Fig. 5 for the location of the nitrogen atom in the crystal structure). In Fig. 8 (d) the empty N(Z+1/2) states with p-character are plotted (blue curve) which correspond to strong NEXAFS signals because of the large matrix element of the 1s - 2p dipole transition. Again, it is obvious that peak B corresponds to the newly created state through the core-hole that is partly hybridized with the LUMO+2 of the complex in the ground-state.

Since we are mostly interested in understanding the different charge transfer in DTBDT-TCNQ with respect to DTBDT-F_4TCNQ we also show in Fig. 9 the DOS comparison in DTBDT-F_4TCNQ. We observe a high similarity of the results in the vicinity of the Fermi energy in the initial state. The excited core hole provokes a similar shift of the higher lying unoccupied states towards the LUMO as in the case of DTBDT-TCNQ. In addition, Fig. 9 (c) shows the unoccupied orbitals localized at the F atom. The contribution of fluorine orbitals to

This manuscript was accepted by J. Chem. Phys. Click here to see the version of record.

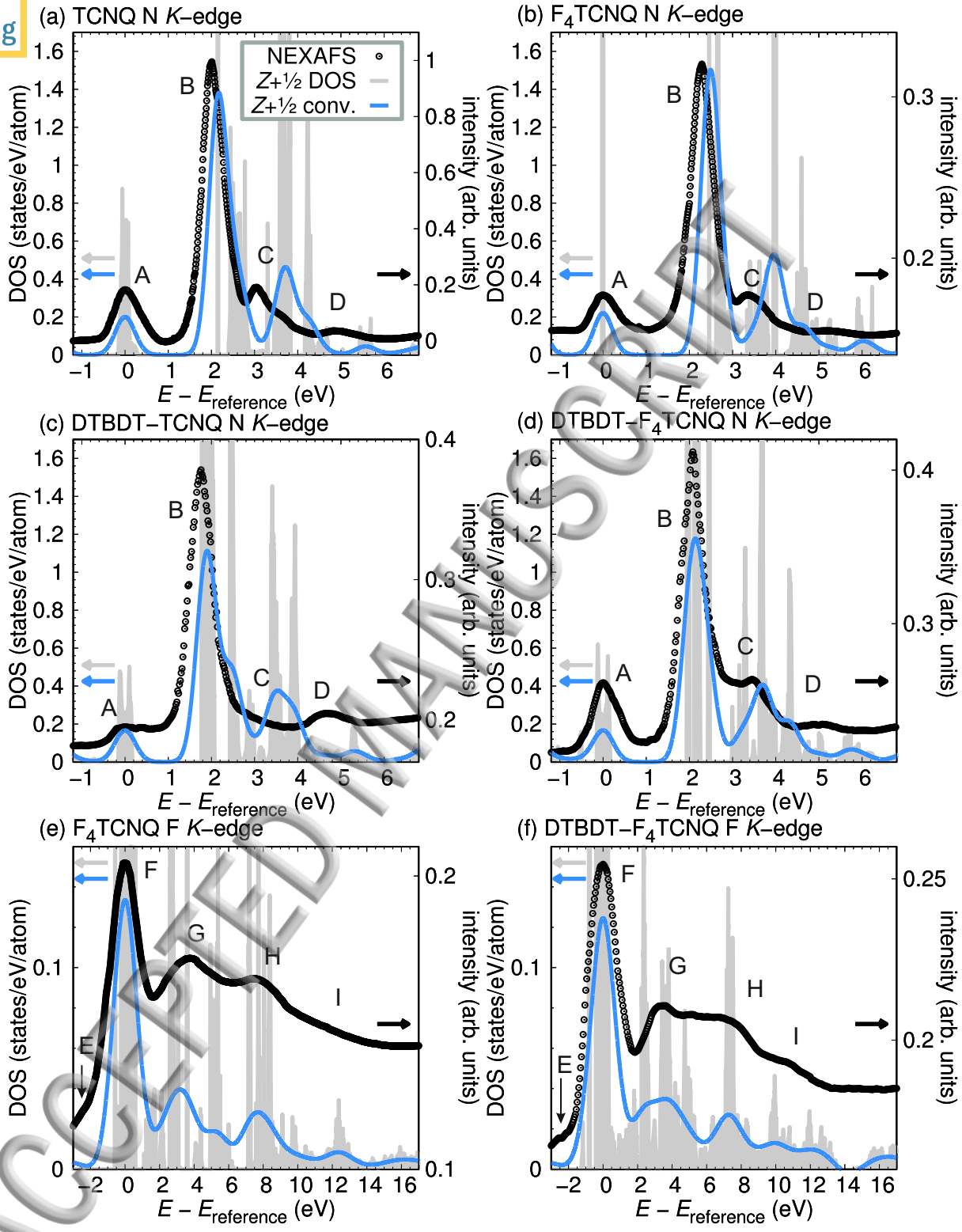

FIG. 7. Nitrogen and fluorine K-edge NEXAFS measurements (black circles) in comparison with calculated results. Grey lines represent the local $2p$ densities of states for the ion with Z increased by 1/2. Blue lines represent the same data, but broadened with $\Gamma = 0.5$ eV for (a) to (d), and with $\Gamma = 1.5$ eV for (e) and (f). Experimental spectra of pure acceptors are scaled to 1 at maximum intensity, spectra of CT compounds have correct relative intensities accordingly. The energy scale is explained in the text.

ACCEPTED MANUSCRIPT

This manuscript was accepted by J. Chem. Phys. Click here to see the version of record.

AIP Publishing

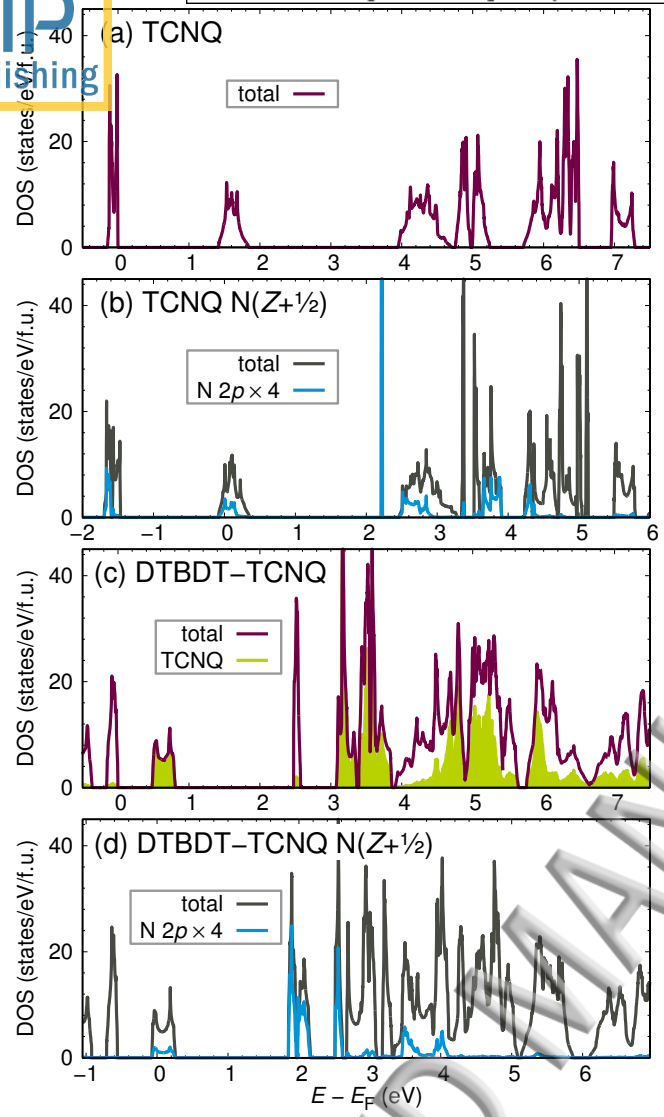

FIG. 8. (a) DOS in TCNQ, (b) DOS in TCNQ with $Z+1/2$ for one nitrogen, (c) DOS in DTBDT-TCNQ (d) DOS in DTBDT-TCNQ $Z+1/2$.

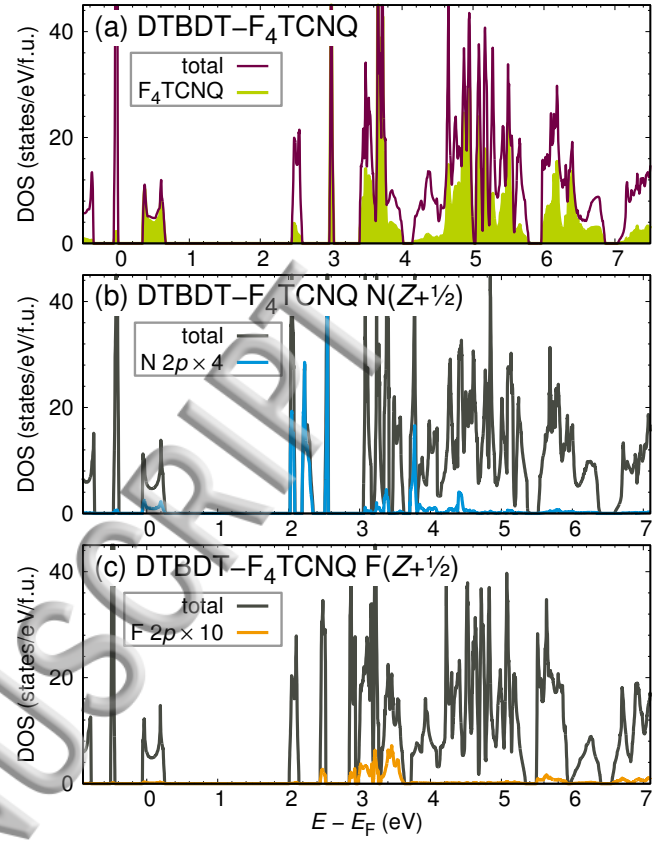

FIG. 9. (a) Density of states in DTBDT-F_4TCNQ, (b) same in DTBDT-F_4TCNQ with $Z+1/2$ for one nitrogen, and (c) same with $Z+1/2$ for one fluorine.

the LUMO is very small.

The good agreement of the main peak positions observed in experiment and theory suggests that for both compounds peak A originates from the LUMO, which is located very close to the Fermi energy. Accordingly, this orbital carries signatures of the charge transfer. The higher lying orbitals (peaks B, C and D) observed in the experiment are apparently shifted to lower energies by the core hole which is only partially screened. In the initial state they are separated from the LUMO by more than 1 eV and it is therefore unlikely that these orbitals take part in the charge transfer process.

For the assignment of the molecular states we have calculated Wannier functions for the conduction band, originating mostly from the LUMO orbital of the acceptor molecules (see Fig. 10). In both compounds, the LUMO orbital is located nearly completely at the acceptor molecule. The theoretical results reveal that changes of the DOS weight of the LUMO comparing pure acceptor molecules with the CT compound are very subtle. This reflects the comparatively small charge transfer of a fraction of an electron per molecule. The absolute value of the charge transfer is in fact slightly larger for the case of F_4TCNQ as also obtained from the calculations (see Table II first column). However, it does not agree with the estimates derived from the IR measurements (see Table II third column). This discrepancy may originate from the maybe too simplified form of Eq. (1) and requires further investigation.

The contribution of the LUMO localized at the nitrogen atom is again a fraction of the total LUMO. Since the fractional core hole does not change the integrated DOS of the LUMO one can also discuss the theoretical results shown in Figs. 7 (a) to (d) comparing the intensities of peak A in the pure acceptor with the mixed compound for the presence of half a core hole.

In DTBDT-TCNQ we observe both in the theoretical prediction and the experimental results that peak A decreases between the pure acceptor and the CT system. In contrast, for DTBDT-F_4TCNQ peak A shows an unexpected relative increase. The reason for this observation

ACCEPTED MANUSCRIPT

This manuscript was accepted by J. Chem. Phys. Click here to see the version of record.

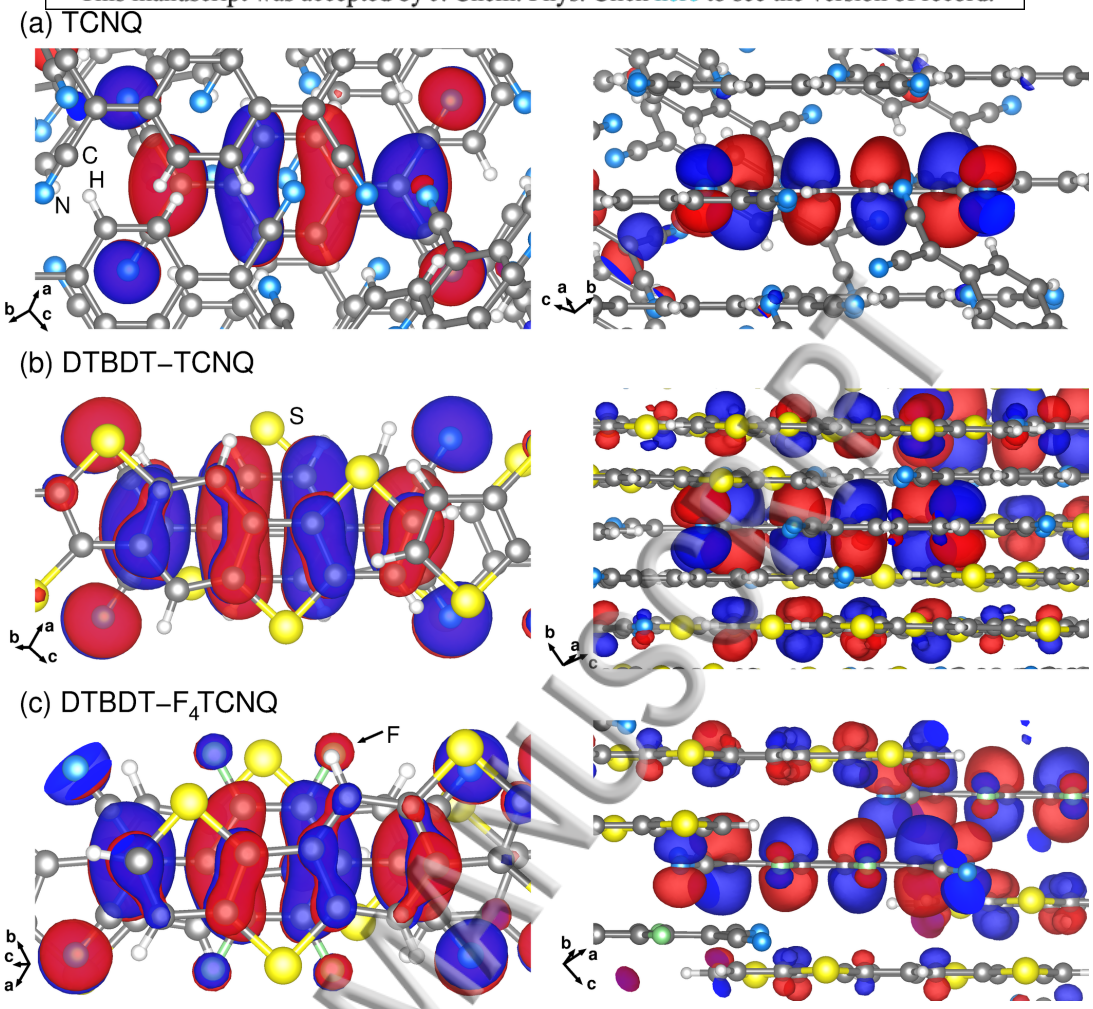

FIG. 10. Wannier functions for the conduction band of (a) TCNQ, (b) DTBDT-TCNQ, and (c) DTBDT-F_4TCNQ. These Wannier functions are similar in shape to the LUMO orbital of TCNQ/F_4TCNQ molecules but have tails reflecting the hybridization of the acceptor molecules in the crystal.

could be a preferential flat orientation of the DTBDT-F_4TCNQ single crystals on the sample holder. Please note, that DTBDT-F_4TCNQ and DTBDT-TCNQ crystals have different macroscopic shapes (see Fig. 1). In this case the assumption of random orientation is not fulfilled and the preferential orientation very likely leads to a different excitation probability into the LUMO state in both compounds.

As the relative peak heights are no longer a conclusive measure of the charge transfer, we discuss in the following the peak widths. Compared to the pure acceptor molecules, peak A broadens in the compounds. In the case of DTBDT-TCNQ, peak A even forms a flat region, while in the case of DTBDT-F_4TCNQ peak A develops a shoulder towards higher photon energy. This directly reflects the theoretical result of a band broadening of the LUMO caused by hybridization. Without considering the lifetime broadening, the calculated LUMO bandwidth for the pure acceptor molecules is about 0.1 eV. For the compounds it increases to 0.2 eV (DTBDT-TCNQ) and 0.3 eV (DTBDT-F_4TCNQ).

More insight into the charge transfer process is gained from the Wannier functions shown in Fig. 10. It can be clearly seen that the LUMO extends to the adjacent donor molecules for both CT compounds. While the amount of intermolecular charge transfer is rather similar for both compounds, the intramolecular charge transfer shows subtle differences. In the case of DTBDT-TCNQ the LUMO shows a larger weight at the cyano groups at both ends of the TCNQ molecule. In the case of DTBDT-F_4TCNQ the LUMO weight is shifted more to the central part of the F_4TCNQ molecule. This might be caused by the strong electronegativity of the four F atoms close to the central part.

For other TCNQ based charge transfer compounds it was proposed that the charge transfer is initiated by charging the cyano groups[60]. These authors give the interpretation that the ionization of the cyano groups aromatizes the central hexagon ring, which can only take place by changing a specific bond from double to sin-

ACCEPTED MANUSCRIPT

This manuscript was accepted by J. Chem. Phys. Click here to see the version of record.

gle. In such a scenario,the extra electron is thus accommodated in one of the cyano groups, so that one of the molecular ends remains radical in character, whereas the other end loses the radicaloid character by accumulating one extra electron. Bond conjugation at the dicyanomethylene ends, however, remains, so that both the extra electron and the radical character are delocalized at each cyano group. As a result one double bond is shifted towards the central ring, which then would lead to the formation of a delocalized (benzene-like) π-state at the central ring. While there is no straightforward interpretation of the shape of the Wannier functions in terms of different types of bonding (single or double bonding), inspection of the calculated Wannier functions Fig. 10 shows that an antisymmetric behavior of the LUMO is conserved for both compounds and no delocalized π state formation at the central ring seems to happen.

Additional support for this explanation can be gained from the fluorine K-edge data. As can be deduced from Fig. 7 (e)-(f), the LUMO shows up as the small signal E at the low-energy onset of the NEXAFS spectrum, giving evidence of a small overlap between F 1s and the LUMO orbital. The same can be deduced from the small intensity of the LUMO (at 0 eV) in the theory spectra (blue curves in (e) and (f)). We also see from Fig. 10 (c) that the LUMO has only a very small contribution located at the fluorine sites.

V. SUMMARY

In summary, we have investigated the charge transfer mechanism in single crystals of recently synthesized DTBDT-TCNQ and DTBDT-F_4TCNQ by considering a combination of near-edge X-ray absorption spectroscopy (NEXAFS) and density functional theory calculations (DFT). We first tested various *ab initio*-based methods in order to have an accurate interpretation of the NEXAFS observations including the *sudden state approximation*, the calculation of the excitation spectrum through time-dependent DFT, the *core-hole approximation* and the *Z+1 or Z+1/2 approximation*. This analysis showed that a description that considers the partial screening of the electron-hole Coulomb correlation on a static level as well as the rearrangement of electronic density (half core-hole approximation) best agrees with the experimental observations and calls for a reinterpretation of previous NEXAFS data on pure TCNQ. Furthermore we showed that almost the same quality of agreement can be obtained by the much faster $Z+1/2$ approximation, where the core hole effects are simulated by replacing N or F with atomic number Z with the neighboring atom with atomic number $Z+1/2$.

Our calculations allowed a unique assignment of the experimentally observed NEXAFS peaks to molecular orbitals. For DTBDT-TCNQ and DTBDT-F_4TCNQ the peak at the lowest excitation energy in the nitrogen and fluorine K-edge spectra were identified as originating from the LUMO orbital. The different behavior of this peak comparing the two compounds indicates that the charge transfer mechanism is modified by the fluorine ligands and the resulting different crystal structure, leading to approximately the same amount of electron transfer, although the acceptor strength of F_4TCNQ is much larger. In particular, we found that while the amount of intermolecular charge transfer is rather similar for both compounds, the intramolecular charge transfer shows some differences that we quantified in terms of LUMO weight distribution. In DTBDT-TCNQ the LUMO has a larger weight at the cyano groups at both ends of the TCNQ molecule while in DTBDT-F_4TCNQ the LUMO weight is shifted to the central region of the F_4TCNQ molecule, which might be caused by the strong electronegativity of the four F atoms close to the central region.

In conclusion, this study (i) sets a reliable and computationally affordable theoretical framework for investigating NEXAFS spectra in molecular crystals and (ii) shows that the charge transfer process in the newly synthesized DTBDT-TCNQ and DTBDT-F_4TCNQ differs only in subtle details.

ACKNOWLEDGMENTS

The project is funded through Transregio SFB TR 49 (Frankfurt, Mainz and Kaiserslautern), Graduate School of Excellence Materials Science in Mainz MAINZ and by Center for Innovative and Emerging Materials (CINEMA), Mainz. A. M. acknowledges funding from the Stiftung Polytechnische Gesellschaft Frankfurt am Main.

In the Supplementary Material the crystal structures of the novel charge transfer complexes are represented as well as the experimental transport data and theoretical calculations for F_4TCNQ.

[1] J. M. Williams, J. R. Ferraro, R. J. Thorn, K. D. Carlson, U. Geiser, H. H. Wang, A. M. Kini, and M.-H. Whangbo, *Organic superconductors (including fullerenes): Synthesis, structure, properties, and theory* (Prentice Hall, Englewood Cliffs, 1992).
[2] K. Kuroki, J. Phys. Soc. Jpn. **75**, 051013 (2006).
[3] H. C. Kandpal, I. Opahle, Y.-Z. Zhang, H. O. Jeschke, and R. Valentí, Phys. Rev. Lett. **103**, 067004 (2009).
[4] N. Toyota, M. Lang, and J. Müller, *Low-Dimensional Molecular Molecules* (Springer-Verlag (Berlin), 2007).
[5] M. M. Alam and S. A. Jenekhe, Chem. Mater. **16**, 4647 (2004).
[6] X. Guo, M. Baumgarten, and K. Müllen, Prog. Polym. Sci. **38**, 1832 (2013).
[7] A. Mishra, C.-Q. Ma, and P. Bäuerle, Chem. Rev. **109**, 1141 (2009).
[8] R. Claessen, M. Sing, U. Schwingenschlögl, P. Blaha, M. Dressel, and C. S. Jacobsen, Phys. Rev. Lett. **88**, 096402 (2002).
[9] M. Sing, U. Schwingenschlögl, R. Claessen, P. Blaha, J. M. P. Carmelo, L. M. Martelo, P. D. Sacramento, M. Dressel, and C. S. Jacobsen, Phys. Rev. B **68**, 125111 (2003).
[10] K. P. Goetz, D. Vermeulen, M. E. Payne, C. Kloc, L. E. McNeil, and O. D. Jurchescu, J. Mater. Chem. C **2**, 3065 (2014).
[11] M. Rudloff, K. Ackermann, M. Huth, H. O. Jeschke, M. Tomic, R. Valentí, B. Wolfram, M. Bröring, M. Bolte, D. Chercka,

ACCEPTED MANUSCRIPT

This manuscript was accepted by J. Chem. Phys. Click here to see the version of record.

AIP Publishing

M. Baumgarten, and K. Müllen, Phys. Chem. Chem. Phys. **17**, 4118 (2015).
[12] E. Mitrany, E. Canadell, and J.-P. Pouget, Europhys. Lett. **113**, 27006 (2016).
[13] P. Gao, D. Beckmann, H. N. Tsao, X. Feng, V. Enkelmann, M. Baumgarten, W. Pisula, and K. Müllen, Adv. Mater. **21**, 213 (2009).
[14] D. Bayer, S. Diehl, M. Baumgarten, K. Muellen, T. Methfessel, and H. J. Elmers, Phys. Rev. B **89**, 075435 (2014).
[15] A. Chernenkaya, K. Medjanik, P. Nagel, M. Merz, S. Schuppler, E. Canadell, J.-P. Pouget, and G. Schönhense, Eur. Phys. J. B **88**, 13 (2015).
[16] M. Sing, J. Meyer, M. Hoinkis, S. Glawion, P. Blaha, G. Gavrila, C. S. Jacobsen, and R. Claessen, Phys. Rev. B **76**, 245119 (2007).
[17] K. Medjanik, D. Chercka, P. Nagel, M. Merz, S. Schuppler, M. Baumgarten, K. Müllen, S. A. Nepijko, H.-J. Elmers, G. Schönhense, H. O. Jeschke, and R. Valenti, J. Am. Chem. Soc. **134**, 4694 (2012), pMID: 22321020.
[18] F. Rochet, F. Bournel, J.-J. Gallet, , G. Dufour, L. Lozzi, and F. Sirotti, J. Phys. Chem. B **106**, 4967 (2002).
[19] T. Miyamoto, Y. Kitajima, H. Sugawara, T. Naito, T. Inabe, and K. Asakura, J. Phys. Chem. C **113**, 20476 (2009).
[20] W. Chen, D. C. Qi, Y. L. Huang, H. Huang, Y. Z. Wang, S. Chen, X. Y. Gao, and A. T. S. Wee, J. Phys. Chem. C **113**, 12832 (2009).
[21] J. Stöhr and R. Jaeger, Phys. Rev. B **26**, 4111 (1982).
[22] J. Stöhr, *NEXAFS spectroscopy* (Springer Series in Surface Science, Springer: Heidelberg, 1992).
[23] J. L. Dehmer and D. Dill, Phys. Rev. Lett. **35**, 213 (1975).
[24] S. Iwata, N. Kosugi, and O. Nomura, Jpn. J. Appl. Phys. **17**, 109 (1978).
[25] J. C. Slater and K. H. Johnson, Phys. Rev. B **5**, 844 (1972).
[26] M. Stener, A. Lisini, and P. Decleva, Chem. Phys. **191**, 141 (1995).
[27] L. Triguero, L. G. M. Pettersson, and H. Ågren, Phys. Rev. B **58**, 8097 (1998).
[28] G. Fronzoni, O. Baseggio, M. Stener, W. Hua, G. Tian, Y. Luo, B. Apicella, M. Alfé, M. de Simone, A. Kivimäki, and M. Coreno, J. Chem. Phys. **141**, 044313 (2014).
[29] D. Prendergast and G. Galli, Phys. Rev. Lett. **96**, 215502 (2006).
[30] X. Gonze, B. Amadon, P.-M. Anglade, J.-M. Beuken, F. Bottin, P. Boulanger, F. Bruneval, D. Caliste, R. Caracas, M. Côté, T. Deutsch, L. Genovese, P. Ghosez, M. Giantomassi, S. Goedecker, D. Hamann, P. Hermet, F. Jollet, G. Jomard, S. Leroux, M. Mancini, S. Mazevet, M. Oliveira, G. Onida, Y. Pouillon, T. Rangel, G.-M. Rignanese, D. Sangalli, R. Shaltaf, M. Torrent, M. Verstraete, G. Zerah, and J. Zwanziger, Comput. Phys. Commun. **180**, 2582 (2009).
[31] P. Giannozzi, S. Baroni, N. Bonini, M. Calandra, R. Car, C. Cavazzoni, D. Ceresoli, G. L. Chiarotti, M. Cococcioni, I. Dabo, A. D. Corso, S. de Gironcoli, S. Fabris, G. Fratesi, R. Gebauer, U. Gerstmann, C. Gougoussis, A. Kokalj, M. Lazzeri, L. Martin-Samos, N. Marzari, F. Mauri, R. Mazzarello, S. Paolini, A. Pasquarello, L. Paulatto, C. Sbraccia, S. Scandolo, G. Sclauzero, A. P. Seitsonen, A. Smogunov, P. Umari, and R. M. Wentzcovitch, J. Phys.: Condens. Matter **21**, 395502 (2009).
[32] K. Gilmore, J. Vinson, E. Shirley, D. Prendergast, C. Pemmaraju, J. Kas, F. Vila, and J. Rehr, Comput. Phys. Commun. **197**, 109 (2015).
[33] P. Hohenberg and W. Kohn, Phys. Rev. **136**, B864 (1964).
[34] W. Kohn and L. J. Sham, Phys. Rev. **140**, A1133 (1965).
[35] J. Fraxedas, Y. J. Lee, I. Jiménez, R. Gago, R. M. Nieminen, P. Ordejón, and E. Canadell, Phys. Rev. B **68**, 195115 (2003).
[36] B. Mahns, O. Kataeva, D. Islamov, S. Hampel, F. Steckel, C. Hess, M. Knupfer, B. Büchner, C. Himcinschi, T. Hahn, R. Renger, and J. Kortus, Cryst. Growth Des. **14**, 1338 (2014).
[37] R. Laudise, C. Kloc, P. Simpkins, and T. Siegrist, J. Cryst. Growth **187**, 449 (1998).
[38] R. E. Long, R. A. Sparks, and K. N. Trueblood, Acta Cryst. **18**, 932 (1965).
[39] T. J. Emge, M. Maxfield, D. O. Cowan, and T. J. Kistenmacher, Mol. Cryst. Liq. Cryst. **65**, 161 (1981).
[40] F. Neese, WIREs Comput. Mol. Sci. **2**, 73 (2012).
[41] A. D. Becke, Phys. Rev. A **38**, 3098 (1988).
[42] A. D. Becke, J. Chem. Phys. **98**, 1372 (1993).
[43] C. Lee, W. Yang, and R. G. Parr, Phys. Rev. B **37**, 785 (1988).
[44] A. Schäfer, H. Horn, and R. Ahlrichs, J. Chem. Phys. **97**, 2571 (1992).
[45] T. H. Dunning, J. Chem. Phys. **90**, 1007 (1989).
[46] P. Blaha, K. Schwarz, G. K. H. Madsen, D. Kvasnicka, and J. Luitz, *WIEN2K, An Augmented Plane Wave + Local Orbitals Program for Calculating Crystal Properties* (Karlheinz Schwarz, Techn. Universität Wien, Austria, 2001).
[47] C. Hébert-Souche, P.-H. Louf, P. Blaha, M. Nelhiebel, J. Luitz, P. Schattschneider, K. Schwarz, and B. Jouffrey, Ultramicroscopy **83**, 9 (2000).
[48] C. Hébert, Micron **38**, 12 (2007).
[49] J. Luitz, M. Maier, C. Hébert, P. Schattschneider, P. Blaha, K. Schwarz, and B. Jouffrey, Eur. Phys. J. B **21**, 363 (2001).
[50] J. P. Perdew, K. Burke, and M. Ernzerhof, Phys. Rev. Lett. **77**, 3865 (1996).
[51] K. Koepernik and H. Eschrig, Phys. Rev. B **59**, 1743 (1999).
[52] Z. Iqbal, C. W. Christoe, and D. K. Dawson, J. Chem. Phys. **63**, 4485 (1975).
[53] J. Robles-Martínez, A. Salmerón-Valverde, J. Argüelles-Ramírez, and A. Zehe, Mol. Eng. **8**, 411 (1999).
[54] P. Pingel, L. Zhu, K. S. Park, J.-O. Vogel, S. Janietz, E.-G. Kim, J. P. Rabe, J.-L. Brédas, and N. Koch, J. Phys. Chem. Lett. **1**, 2037 (2010).
[55] A. Salmerón-Valverde, J. Robles-Martínez, J. García-Serrano, R. Gómez, R. Ridaura, M. Quintana, and A. Zehe, Mol. Eng. **8**, 419 (1999).
[56] M. Meneghetti and C. Pecile, J. Chem. Phys. **84**, 4149 (1986).
[57] E. Runge and E. K. U. Gross, Phys. Rev. Lett. **52**, 997 (1984).
[58] M. A. Marques, N. T. Maitra, F. M. Nogueira, E. Gross, and A. Rubio, *Fundamentals of Time-Dependent Density Functional Theory* (Springer-Verlag Berlin Heidelberg, 2012).
[59] F. M. F. deGroot, R. K. Hocking, C. Piamonteze, B. Hedman, K. O. Hodgson, and E. I. Solomon, AIP Conf. Proc. **882**, 123 (2007).
[60] T.-C. Tseng, C. Urban, Y. Wang, R. Otero, S. L. Tait, M. Alcami, D. Ecija, M. Trelka, J. M. Gallego, N. Lin, M. Konuma, U. Starke, A. Nefedov, A. Langner, C. Wöll, M. A. Herranz, F. Martin, N. Martin, K. Kern, and R. Miranda, Nat. Chem. **2**, 374 (2010).

ACCEPTED MANUSCRIPT

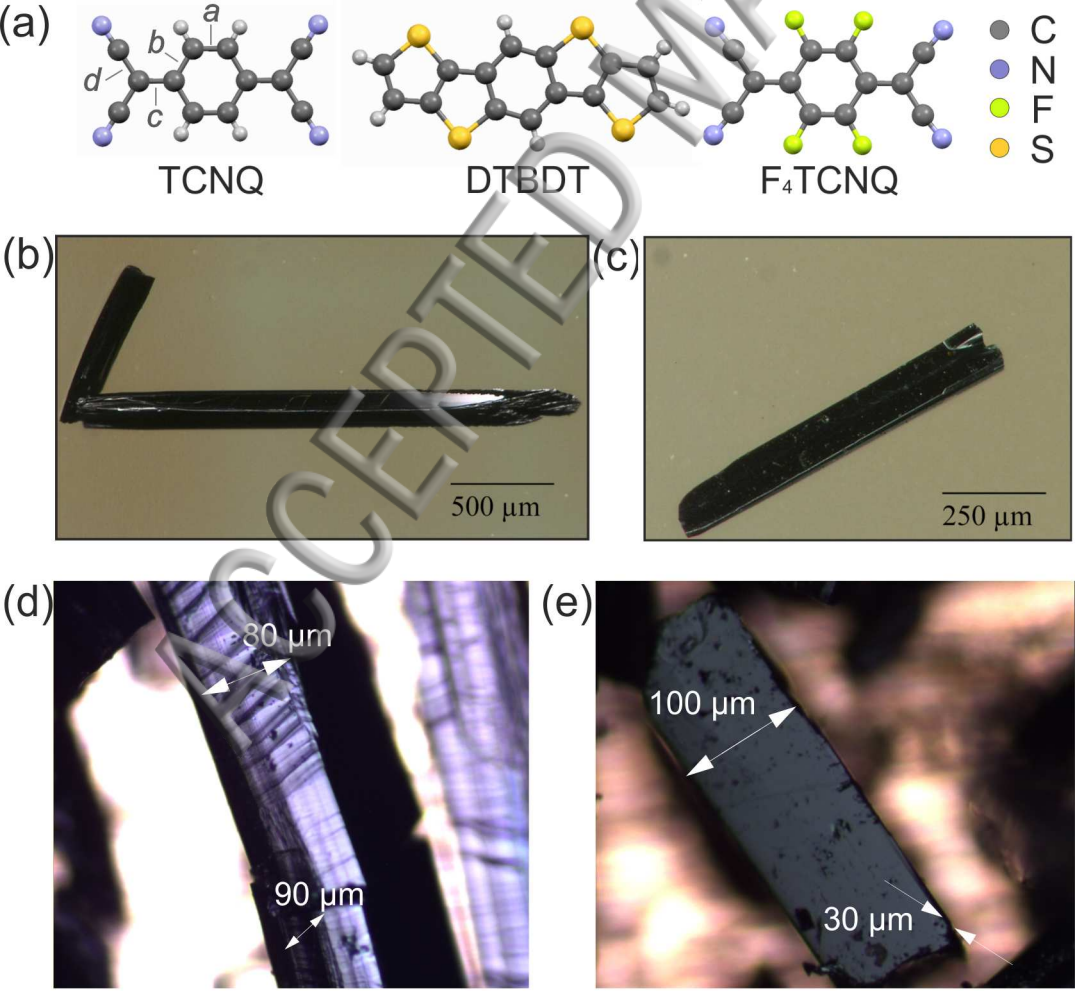

ACCEPTED MANUSCRIPT

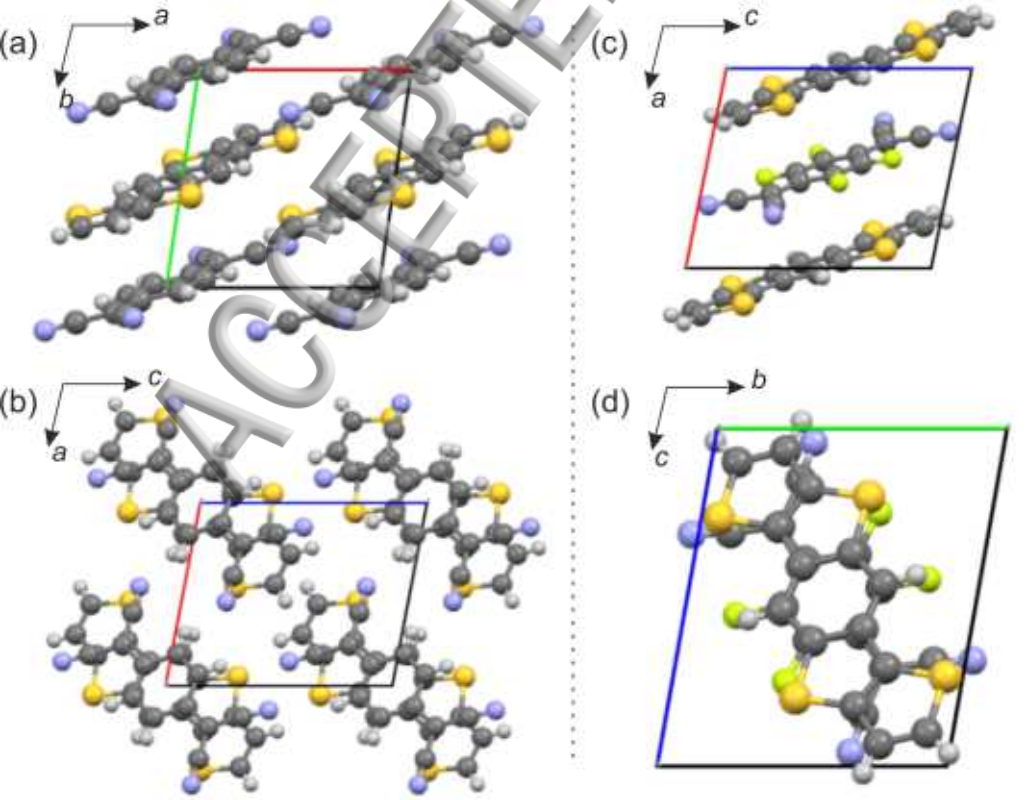

ACCEPTED

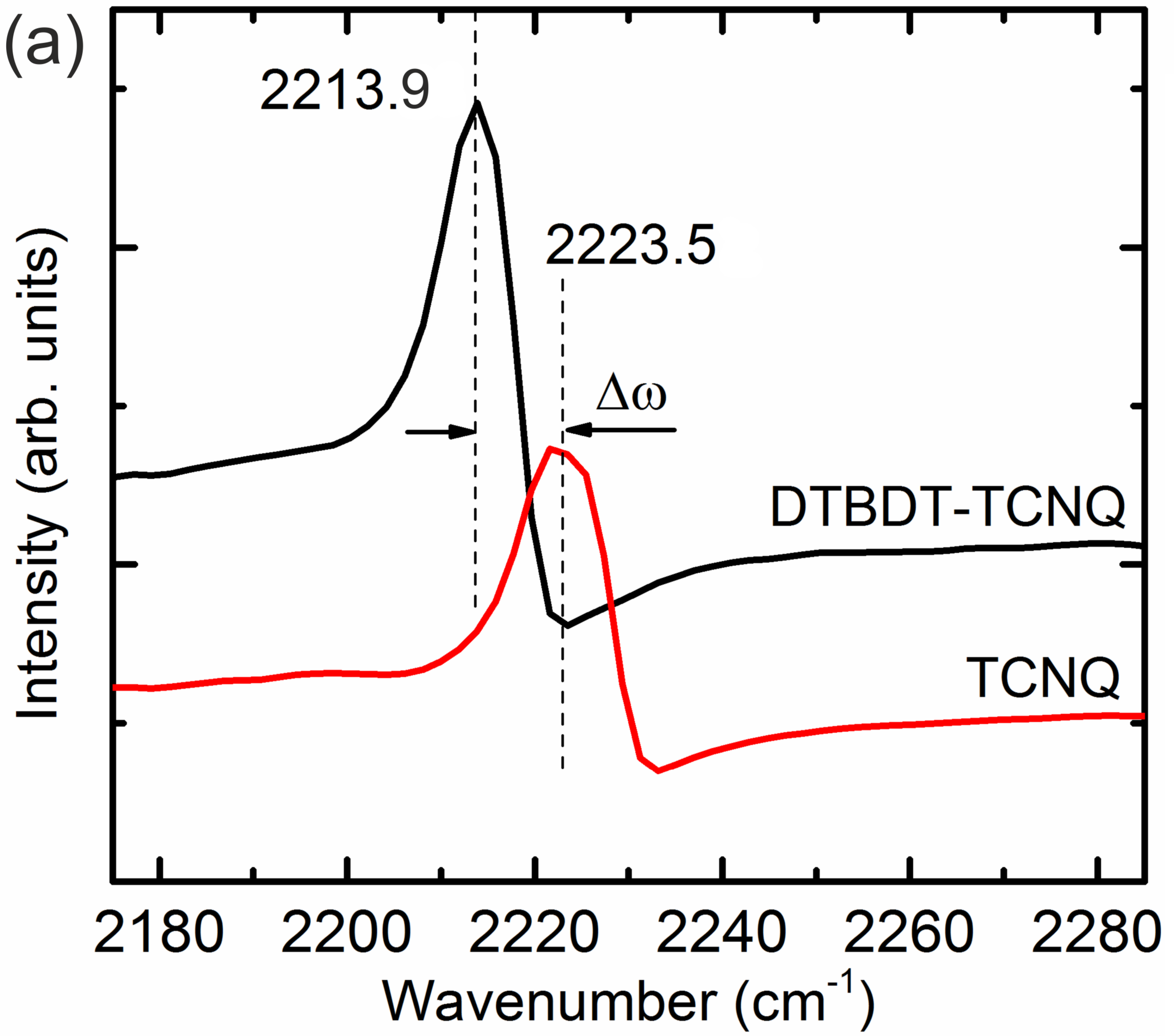

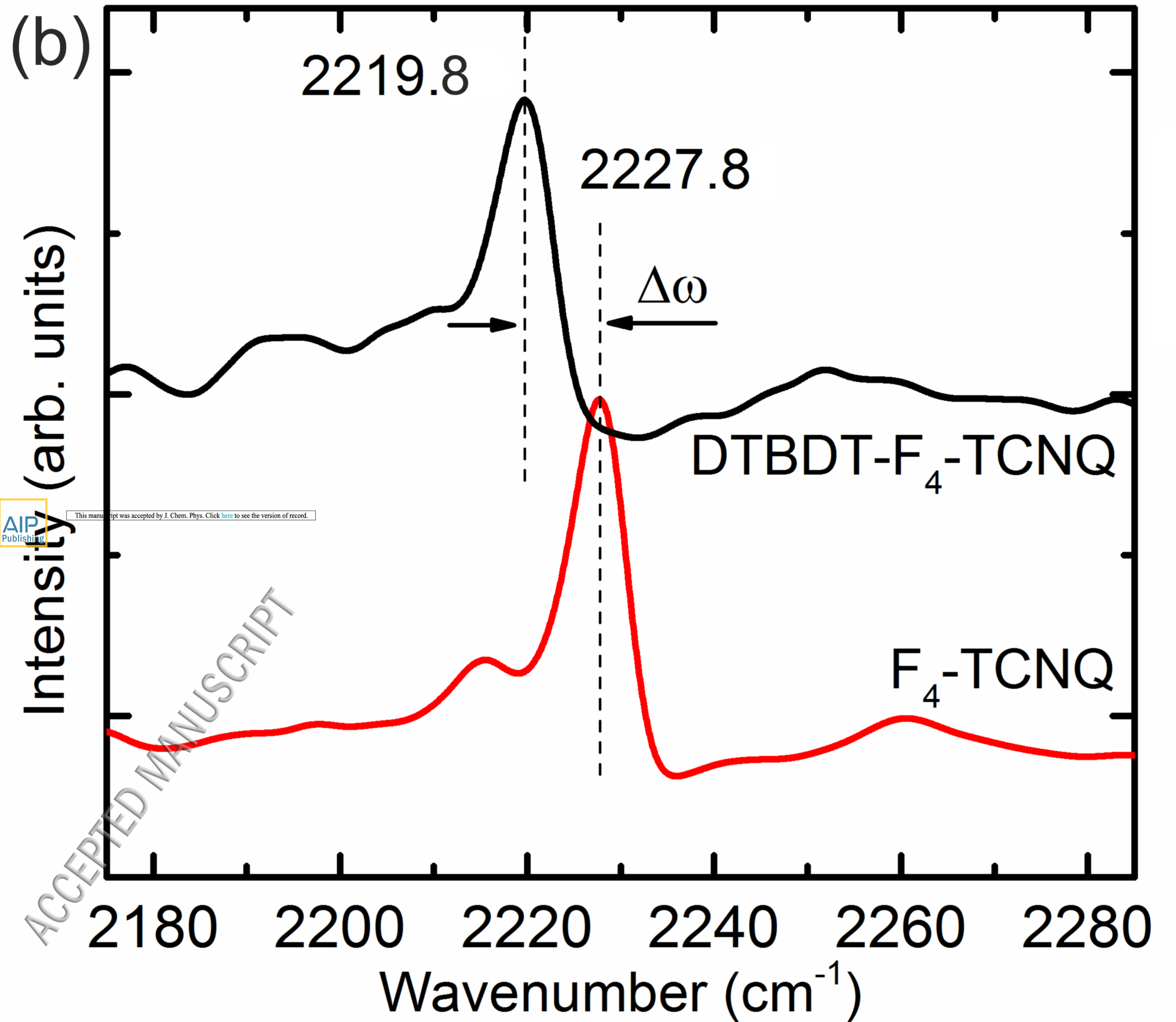

This manuscript was accepted by J. Chem. Phys. Click here to see the version of record.
AIP Publishing
ACCEPTED MANUSCRIPT

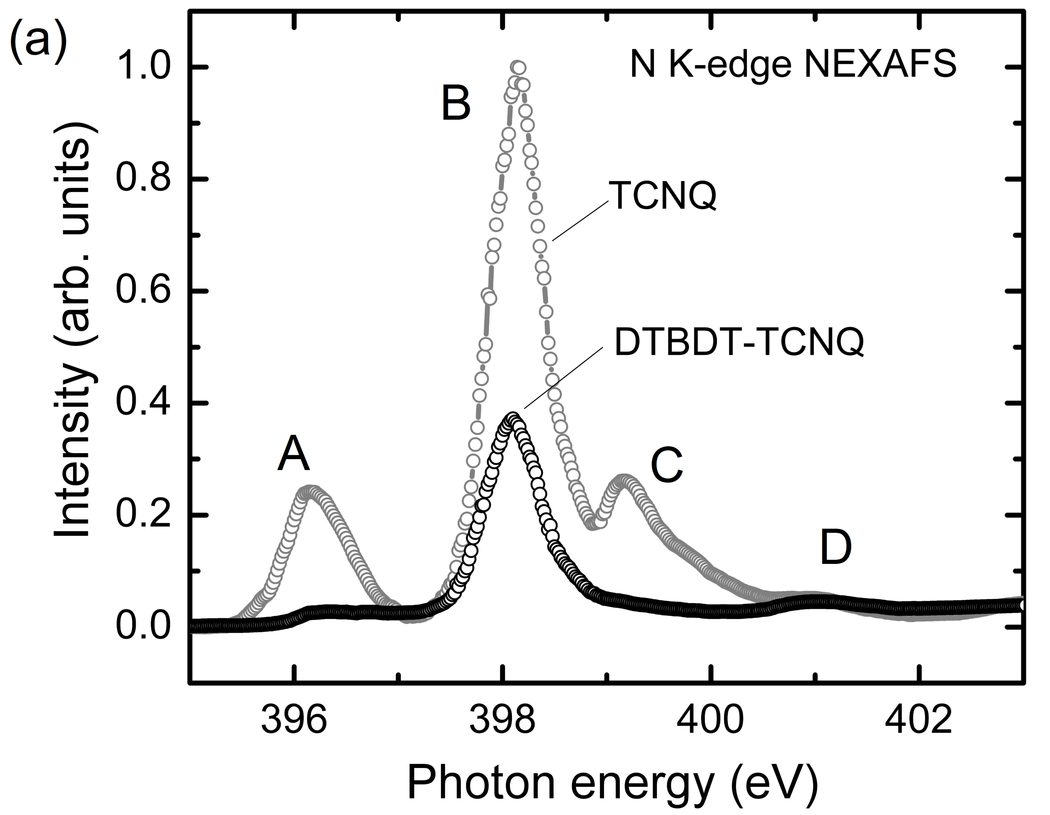

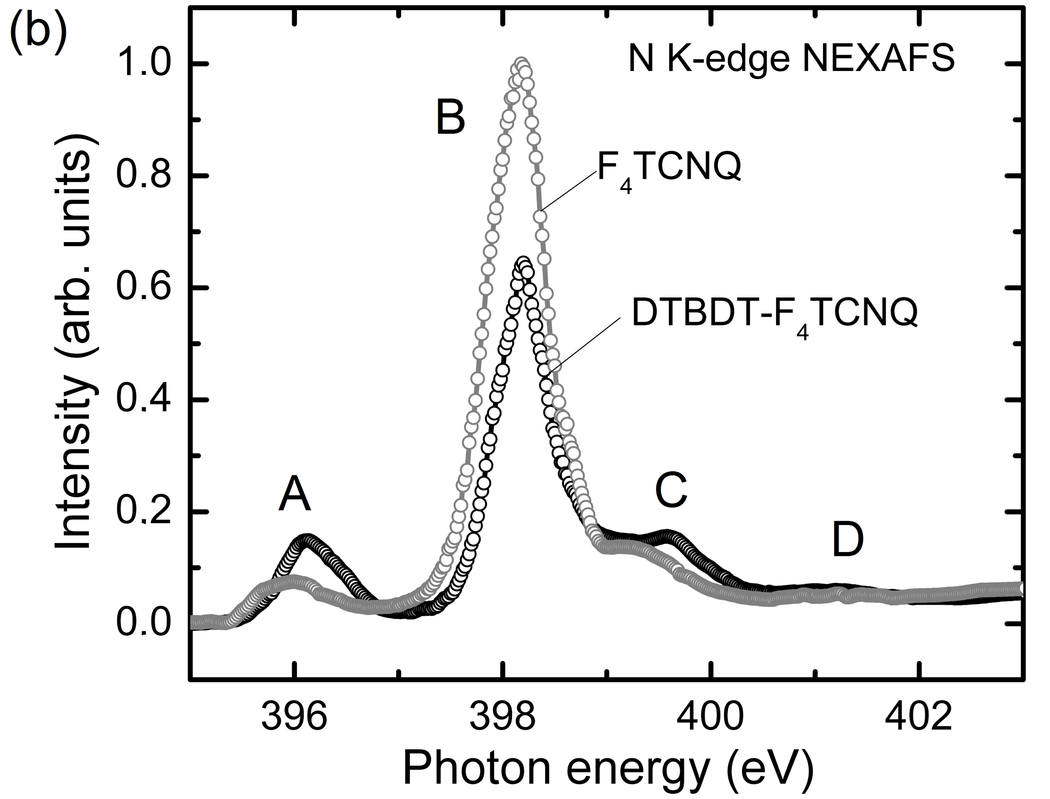

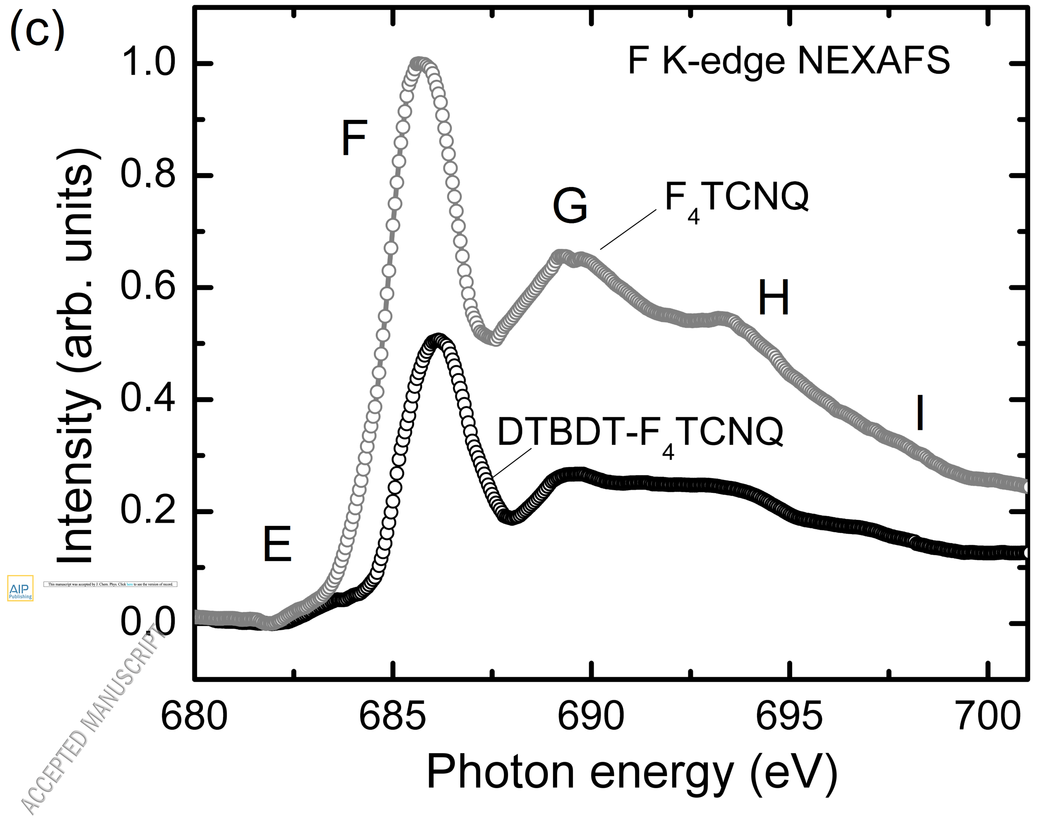

ACCEPTED MANUSCRIPT

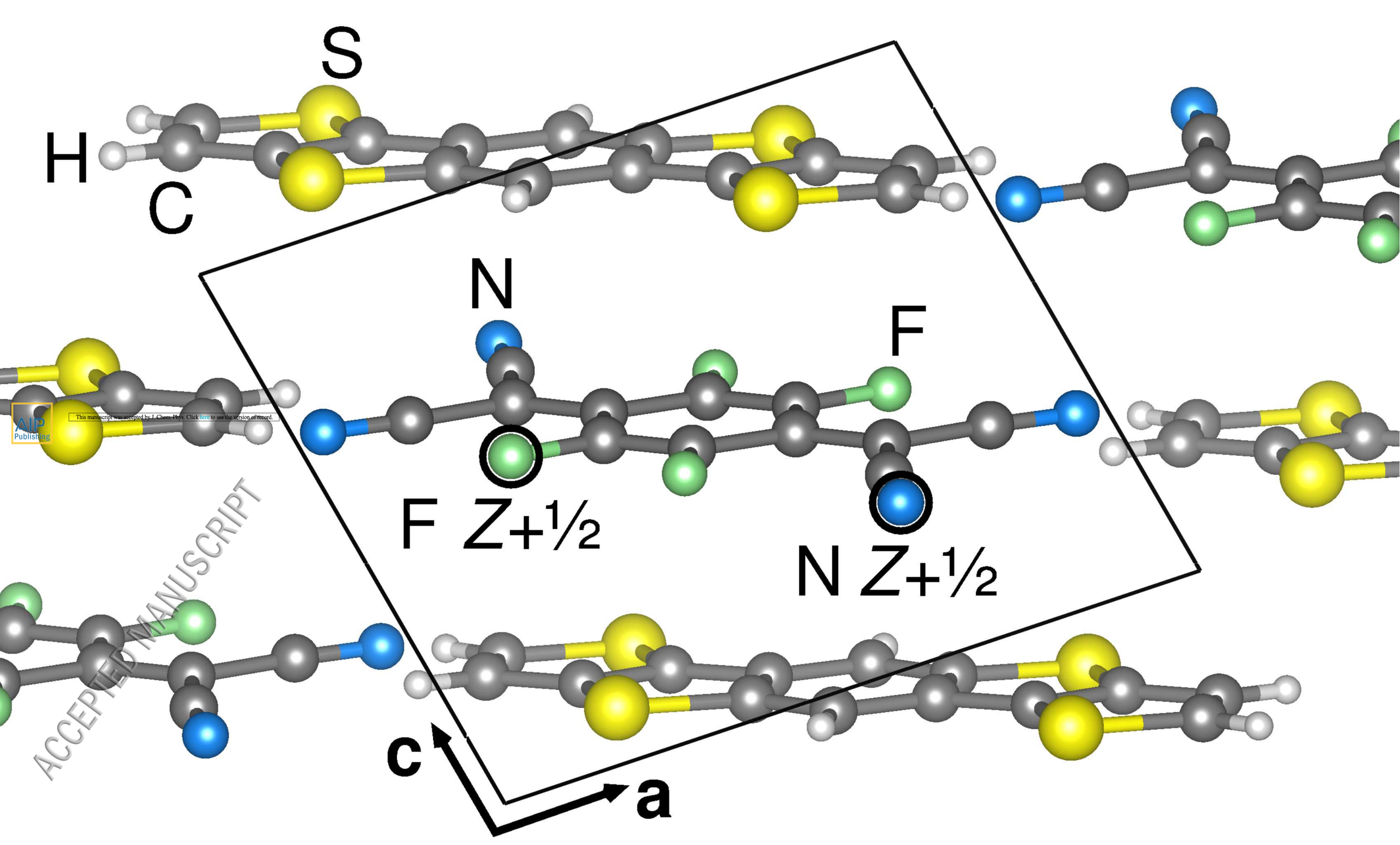

This manuscript was accepted by J. Chem. Phys. Click here to see the version of record.
AIP Publishing
ACCEPTED MANUSCRIPT

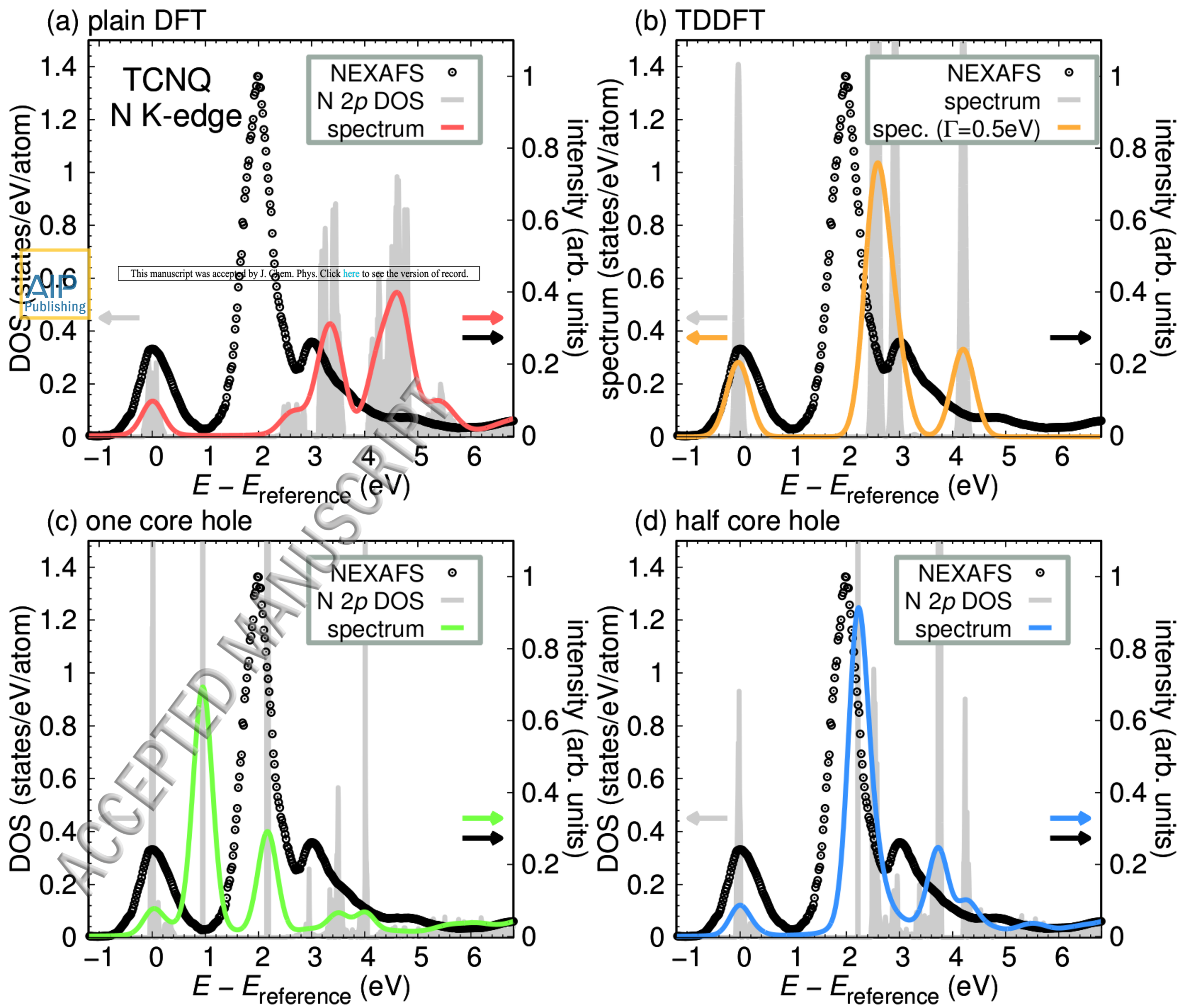

This manuscript was accepted by J. Chem. Phys. Click here to see the version of record.
AIP Publishing
ACCEPTED MANUSCRIPT

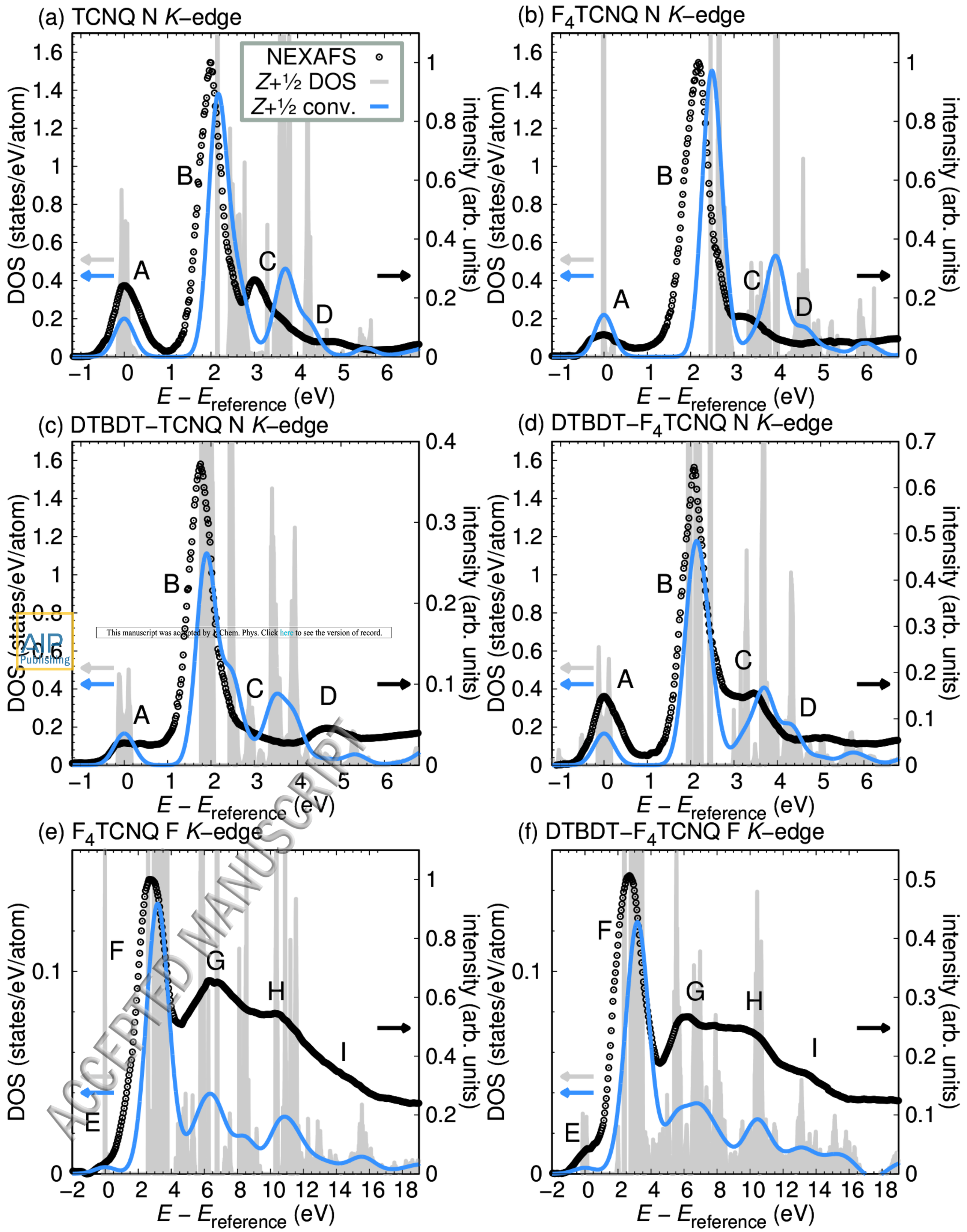

This manuscript was accepted by J. Chem. Phys. Click here to see the version of record.
AIP Publishing
ACCEPTED MANUSCRIPT

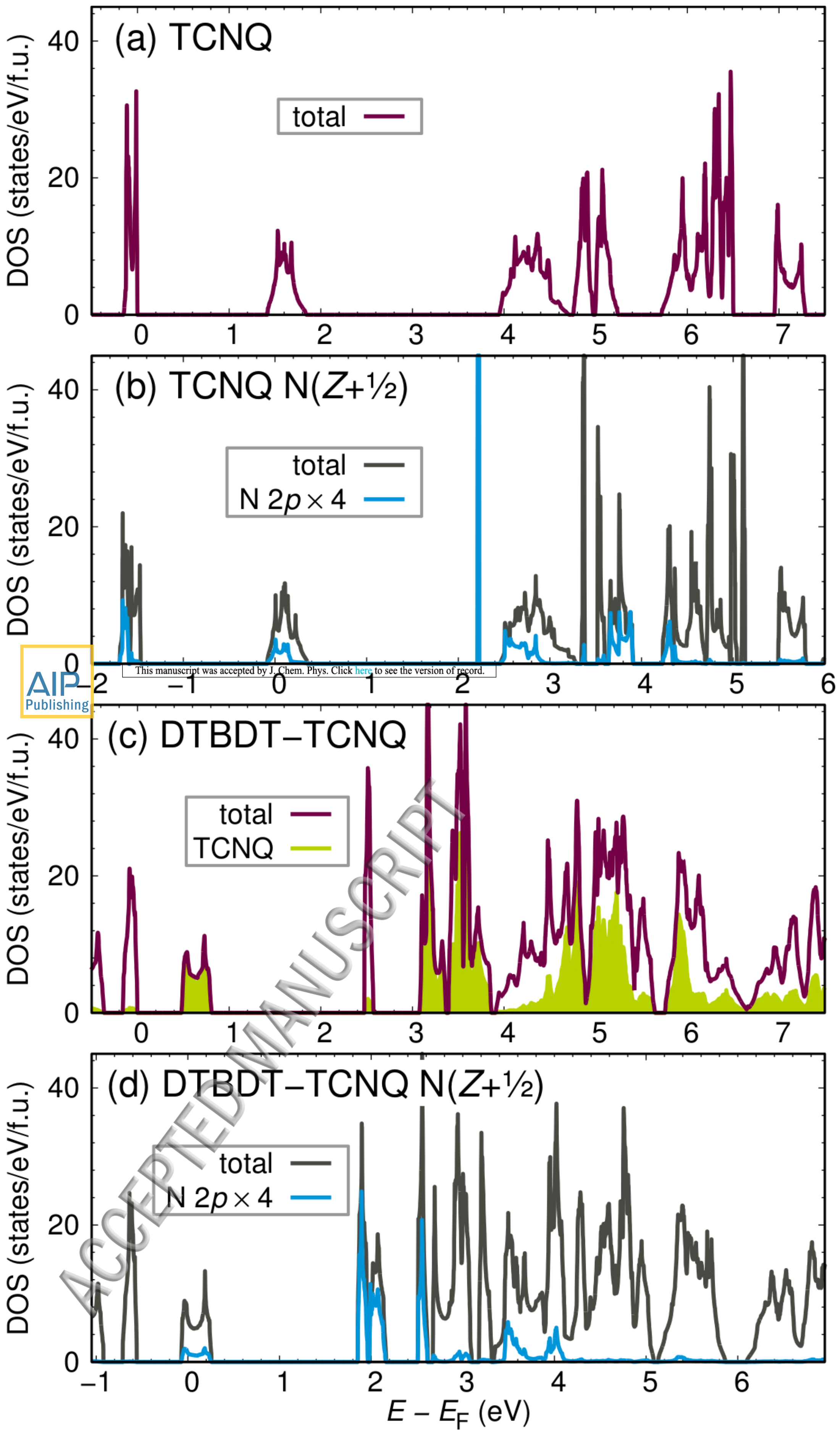

This manuscript was accepted by J. Chem. Phys. Click here to see the version of record.
AIP Publishing
ACCEPTED MANUSCRIPT

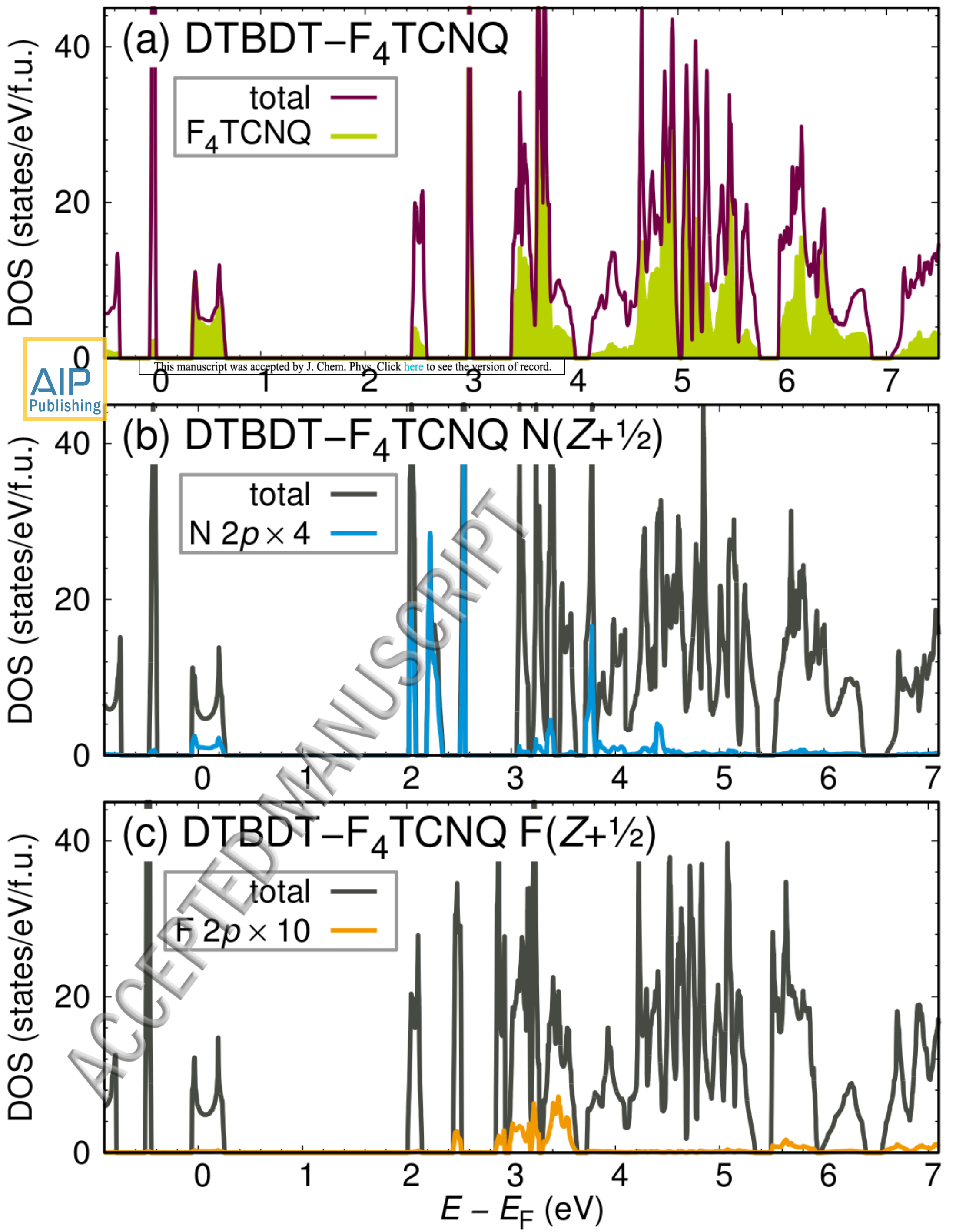

This manuscript was accepted by J. Chem. Phys. Click here to see the version of record.
AIP Publishing
ACCEPTED MANUSCRIPT

(a) TCNQ

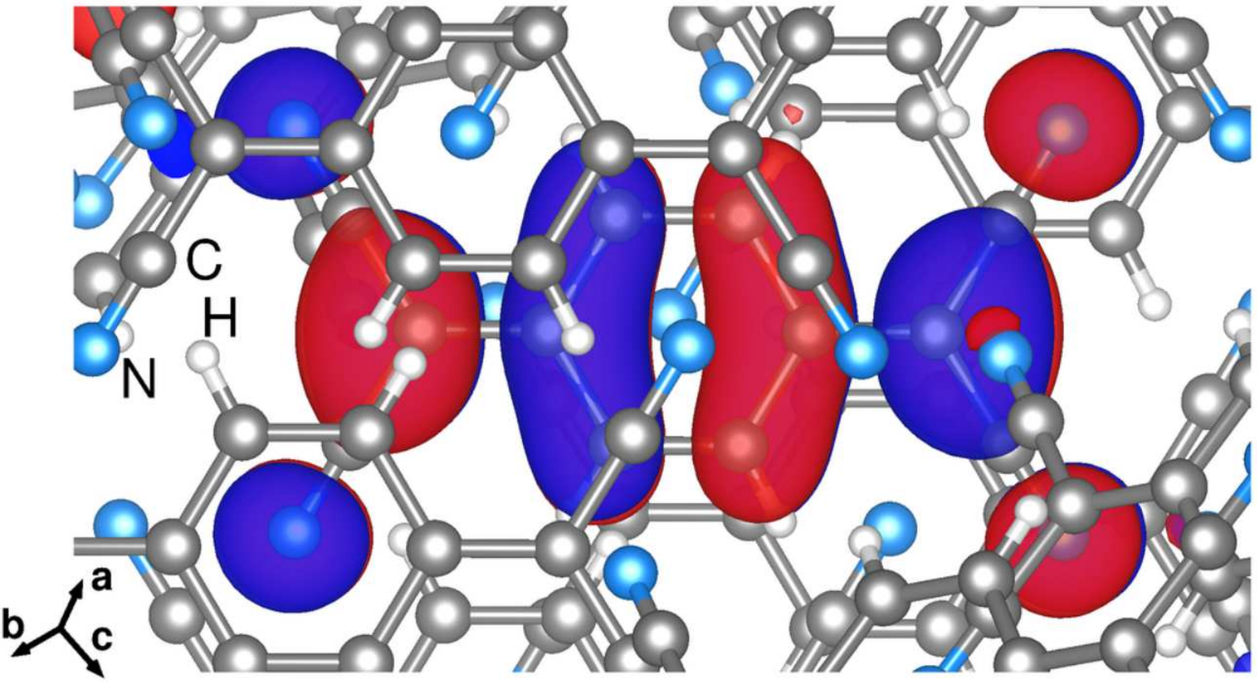

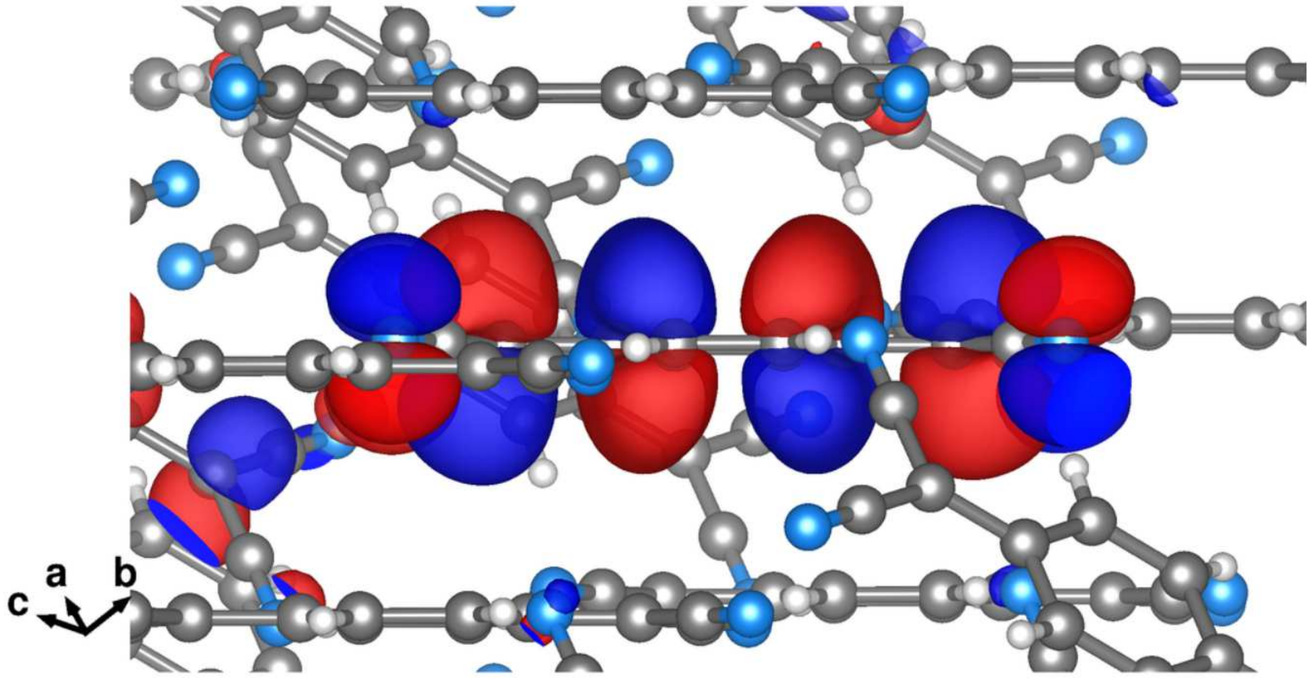

(b) DTBDT–TCNQ

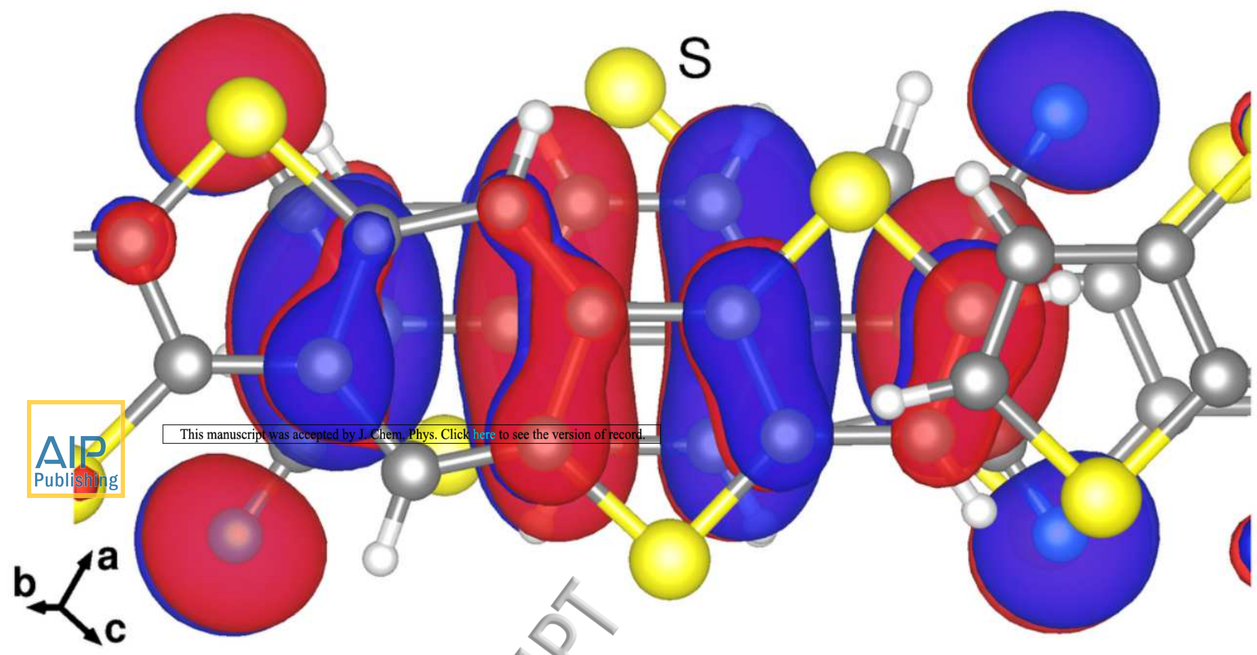

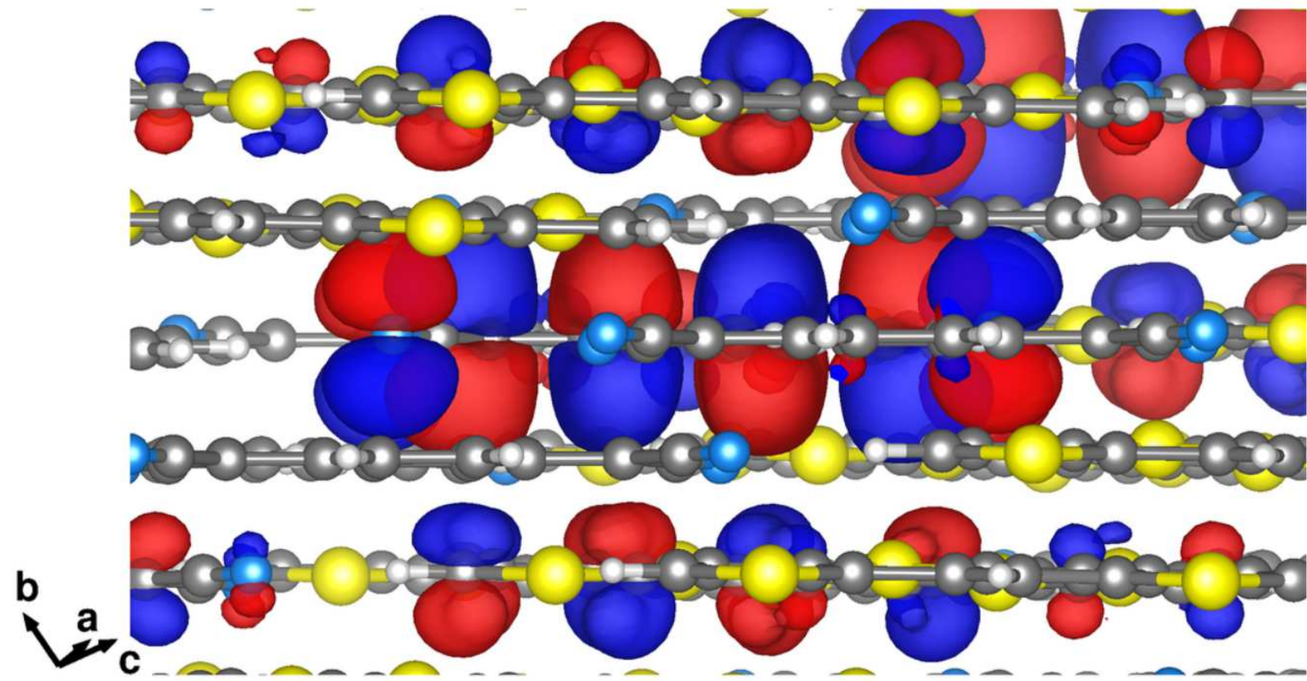

AIP Publishing
This manuscript was accepted by J. Chem. Phys. Click here to see the version of record.

(c) DTBDT–F_4TCNQ

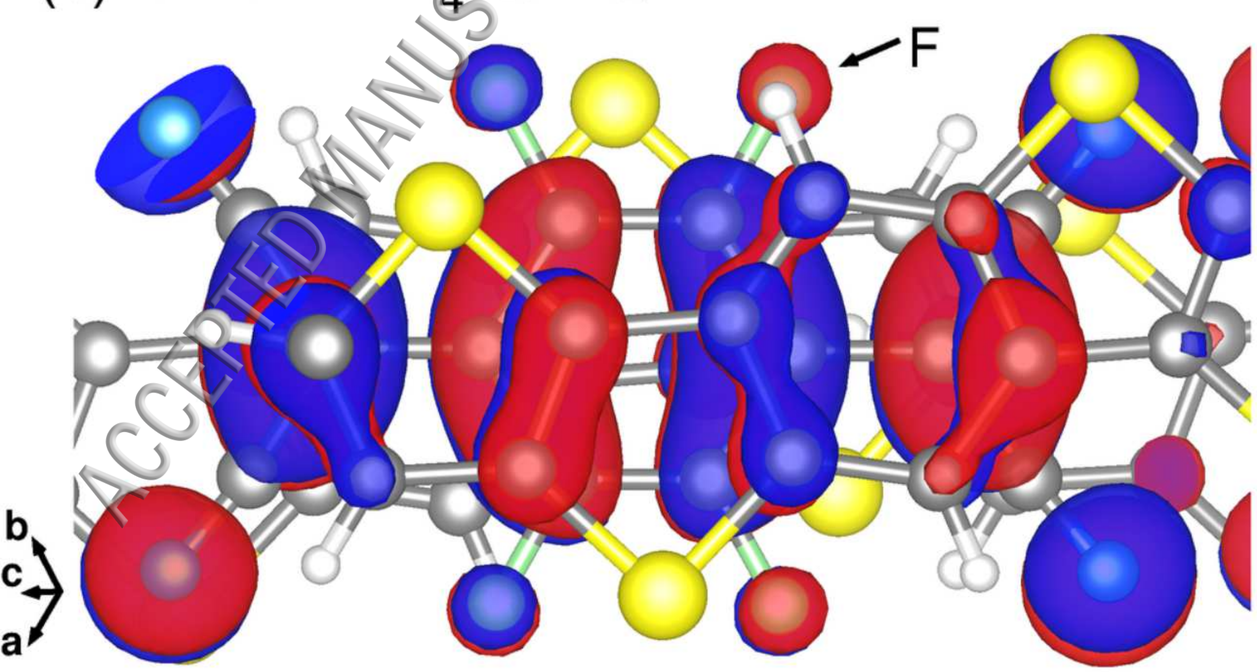

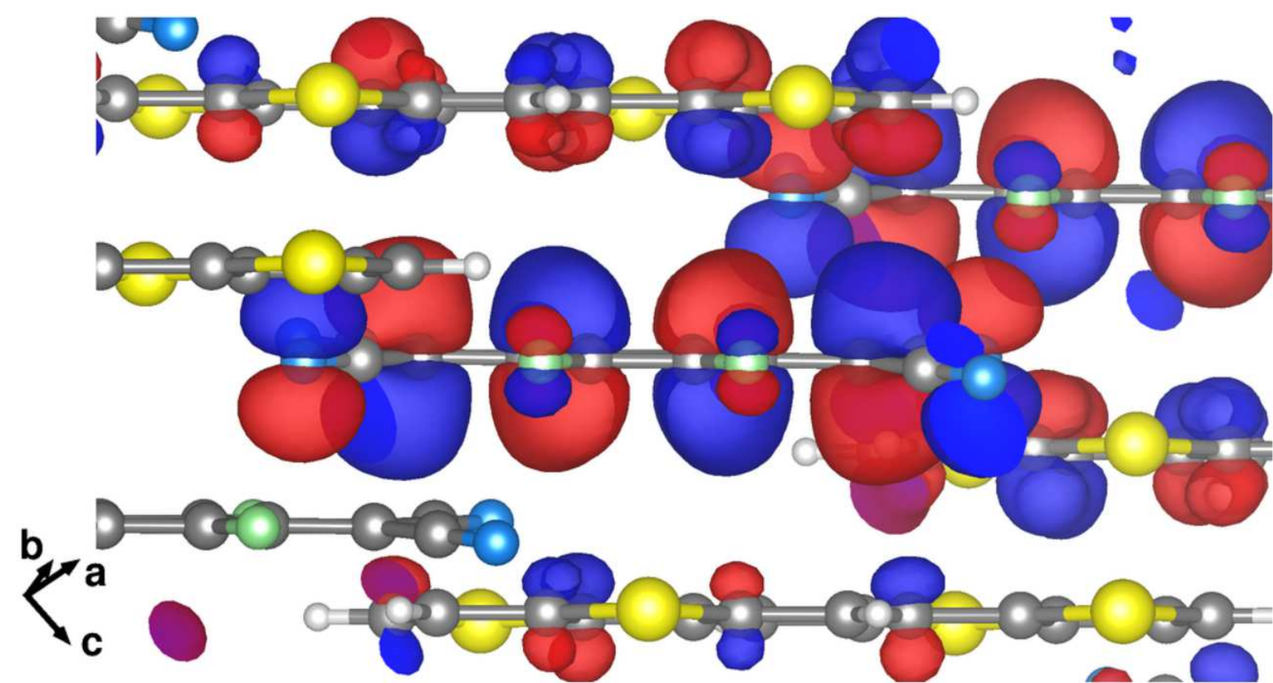

ACCEPTED MANUSCRIPT